Mycobacterium trehalose polyphleates are required for infection by therapeutically useful mycobacteriophages BPs and Muddy

Running title: Phage requirement for trehalose polyphleates

Katherine S. Wetzel[1#], Morgane Illouz[2#], Lawrence Abad[1], Haley G. Aull[1], Daniel A. Russell[1], Rebecca A. Garlena[1], Madison Cristinziano[1], Silke Malmsheimer[2], Christian Chalut[3], Graham F. Hatfull[1*], and Laurent Kremer[2,4*]

[1]Department of Biological Sciences University of Pittsburgh, Pittsburgh, PA 15260 USA

[2]Centre National de la Recherche Scientifique UMR 9004, Institut de Recherche en Infectiologie de Montpellier (IRIM), Université de Montpellier, 1919 route de Mende, 34293, Montpellier, France.

[3]Institut de Pharmacologie et de Biologie Structurale, Université de Toulouse, CNRS, UPS, Toulouse, France

[4]INSERM, IRIM, Montpellier, France

[#]Authors contributed equally

Corresponding authors: gfh@pitt.edu; laurent.kremer@irim.cnrs.fr

Abstract

Mycobacteriophages are good model systems for understanding their bacterial hosts and show promise as therapeutic agents for nontuberculous mycobacterium infections. However, little is known about phage recognition of *Mycobacterium* cell surfaces, or mechanisms of phage resistance. We show here that surface-exposed trehalose polyphleates (TPPs) are required for infection of *Mycobacterium abscessus* and *Mycobacterium smegmatis* by clinically useful phages BPs and Muddy, and that TPP loss leads to defects in adsorption, infection, and confers resistance. Transposon mutagenesis indicates that TPP loss is the primary mechanism for phage resistance. Spontaneous phage resistance occurs through TPP loss, and some *M. abscessus* clinical isolates are phage-insensitive due to TPP absence. Both BPs and Muddy become TPP-independent through single amino acid substitutions in their tail spike proteins, and *M. abscessus* mutants resistant to TPP-independent phages reveal additional resistance mechanisms. Clinical use of BPs and Muddy TPP-independent mutants should preempt phage resistance caused by TPP loss.

54 **Introduction**

55

56 Nontuberculous mycobacteria (NTM) include several important human pathogens such as
57 *Mycobacterium abscessus* and *Mycobacterium avium*[1,2]. These infections are often refractory to
58 effective antibiotic treatment due to both intrinsic and acquired resistance mutations, and new
59 treatment options are needed[3]. The therapeutic application of mycobacteriophages shows some
60 promise for the treatment of pulmonary infections in persons with cystic fibrosis[4-6], disseminated
61 infection following bilateral lung transplantation[4], and disseminated *Mycobacterium chelonae*
62 infection[7]. However, broadening therapy beyond single-patient compassionate use applications
63 will require expansion of the repertoire of therapeutically useful phages, and increasing host
64 range such that a higher proportion of clinical isolates can be treated[5,8,9]. Clinical administration
65 of bacteriophages is anticipated to give rise to phage resistant mutants and disease
66 recurrence[10], but the frequency and mechanisms of mycobacteriophage resistance are poorly
67 understood[11]. Very few mycobacteriophage receptors are known, although glycopeptidolipids
68 (GPLs) are proposed as receptors for mycobacteriophage I3 in *Mycobacterium smegmatis*[12].

69

70 Over 12,000 individual mycobacteriophages have been described, with most being isolated on
71 *M. smegmatis*[13]. The genome sequences of 2,200 of these show them to be highly diverse
72 genetically and pervasively mosaic[14,15]. They can be sorted into groups of genomically related
73 phages (e.g. Cluster A, B, C etc.), some of which can be readily divided into subclusters (e.g.
74 Subcluster A1, A2, A3 etc.) based on sequence variation[16,17]. Seven of the sequenced phages
75 currently have no close relatives and are designated as 'Singletons'. A subset of these phages
76 has relatively broad host range and are also able to efficiently infect *Mycobacterium*
77 *tuberculosis*, including phages in Clusters/Subclusters A2, A3, G1, K1, K2, K3, K4, and AB[18,19].
78 A similar subset of phages also infects some clinical isolates of *M. abscessus*, although it is
79 noteworthy that phage host ranges on these strains is highly variable (even for related phages

80 within clusters/subclusters), and is highly variable among different clinical isolates[4,9]. There is
81 also substantial variation in the outcomes of phage infection of *M. abscessus* strains, with
82 notable differences between rough and smooth colony morphotypes[9]. For example, a smaller
83 proportion of smooth isolates are susceptible to phage infection than rough strains – as
84 determined by plaque formation – and none of the smooth strains are efficiently killed by any
85 phage tested[9].
86
87 Mycobacterial cell walls characteristically have a mycolic acid-rich outer layer referred to as the
88 mycobacterial outer membrane or mycomembrane[20]. In addition to abundant mycolic acids,
89 there are numerous other types of complex molecules including multiple acylated lipids such as
90 di- and polyacyltrehalose (DAT and PAT), phthiocerol dimycocerosate (PDIM) and
91 sulfoglycolipids (SGL), although not all are found in all *Mycobacterium* species. Smooth strains
92 of *M. abscessus* have abundant GPLs although these are lacking or greatly less abundant in
93 rough strains[21,22]. Recently, it has been shown that some mycobacterial species, including *M.*
94 *abscessus*, have trehalose polyphleates (TPPs), which are high-molecular-weight, surface-
95 exposed glycolipids, in their cell walls[23,24]. These TPPs may be important for *M. abscessus*
96 virulence and are associated with clumping and cording[24]. A five gene cluster, – including a
97 polyketide synthetase (Pks) – is required for TPP biosynthesis and TPP precursor (DAT)
98 transport to the outer surface of the cell by MmpL10[25]. TPPs are not present in *M. tuberculosis*
99 although DAT and PAT are[25]. The specific roles of TPPs are not known, but their position on the
100 outer surface makes them candidates for use as phage receptors.
101
102 Here, we show that TPPs are required for the binding and infection of *M. abscessus* by phages
103 BPs and Muddy. These phages share little or no nucleotide similarity but both have been used
104 therapeutically, sometimes in combination with each other[4,26]. *M. abscessus* transposon
105 insertion mutants that are resistant to these phages map in all five genes involved in TPP

106 synthesis, all have lost TPPs from their cell walls, and phage adsorption is lost. Spontaneous
107 phage resistant mutants of some *M. abscessus* clinical isolates also have mutations in the
108 known TPP synthesis genes, and some *M. abscessus* clinical isolates that are insensitive to
109 BPs and Muddy are naturally defective in TPPs. However, the TPP requirement can be readily
110 overcome by mutations in phage tail spike proteins, suggesting that TPPs are acting as a co-
111 receptor, and the cell wall binding target of the phages is likely essential for mycobacterial
112 viability. *M. abscessus* strains resistant to BPs and Muddy TPP-independent mutants reveal
113 new mechanisms of phage resistance.
114
115 **Results**
116
117 **Development of a transposon system for mutagenesis of *M. abscessus* clinical isolates**
118
119 *M. abscessus* GD01 (subspecies *massiliense*) was selected for transposon mutagenesis as it is
120 the first clinical isolate treated therapeutically[4] and is killed well by phages Muddy, ZoeJΔ*45*,
121 and BPsΔ*33*HTH_HRM10, mapping in Clusters AB, K2, and G1, respectively. Muddy is a lytic
122 phage and ZoeJΔ*45* and BPsΔ*33*HTH_HRM10 are engineered lytic derivatives of ZoeJ[27] and
123 BPs[28], respectively. Because GD01 – like many *M. abscessus* isolates – is kanamycin resistant
124 (MIC>128 µg/mL)[29], we re-engineered the extant Kan^R MycoMarT7 transposon using CRISPY-
125 BRED[30] to include a Hyg^R cassette, constructing derivatives both with and without the existing
126 R6Kγ origin of replication (Fig. 1A). The shorter transposon (MycoMarT7-Hyg2) transduced
127 strain GD01 ~100 times more efficiently than the longer MycoMarT7-Hyg1 transposon; this
128 efficiency difference was not observed for *M. smegmatis*. We transduced strain GD01 with
129 MycoMarT7-Hyg2 and selected Hyg-resistant transductants on solid media to yield a random
130 mutagenesis library (Fig. 1B). We note that the parent of the transposon delivery phages, TM4,

131 does not form plaques on any *M. abscessus* strain[9] but efficiently delivers DNA to *M. abscessus*
132 cells[31].
133
134 **BPsΔ*33*HTH_HRM10 and Muddy Tn resistant mutants are defective in trehalose**
135 **polyphleates**
136
137 To identify *M. abscessus* GD01 phage resistant mutants, the Tn library was plated on solid
138 media seeded with either BPsΔ*33*HTH_HRM10 or Muddy. Single colonies were recovered at a
139 frequency of ~10^{-3} and twenty individual colonies were picked from each selection, rescreened,
140 and characterized (Fig. 1, Fig. S1, Table S1). Eighteen of the 20 BPsΔ*33*HTH_HRM10 resistant
141 candidates were mapped, all of which have transposon insertions in a gene cluster involved in
142 trehalose polyphleates synthesis; some appear have secondary transposon insertions mapping
143 elsewhere (Table S1, Fig. 1C, D). Thirteen of the 20 Muddy resistant candidates were mapped
144 and surprisingly all also contain insertions in TPP synthesis genes (Table S1, Fig. 1C, D). TPP
145 synthesis has previously been reported to be non-essential[32], and these observations suggest
146 that loss of TPPs is the primary mechanism of resistance to both BPsΔ*33*HTH_HRM10 and
147 Muddy. Further analysis showed that all of the mutants tested have similar phenotypes with a
148 large reduction in the efficiency of plaquing (EOP) of BPsΔ*33*HTH_HRM10, and a more modest
149 reduction in EOP of Muddy, but with formation of very turbid plaques (Fig. 1E).
150 Complementation of a f*adD23* Tn mutant confirmed that phage resistance results from TPP loss
151 (Fig. 1F). All of the strains that we tested remain sensitive to ZoeJΔ*43-45*, Itos, and Faith1Δ*38-*
152 *40* (Fig. 1E, S1).
153
154 Analysis of cell wall lipids shows that all of the mutants tested have lost TPPs (Fig. 1G).
155 Interruption of TPP precursor transport (as in an *mmpL10* mutant; Fig. 1D), or loss of PE which

156 is needed for the final step of TPP synthesis (Fig. 1D) can result in accumulation of the DAT
157 precursor[23,25], and our *mmpL10* transposon insertion mutants do accumulate DAT. Our *pE*
158 mutants did not accumulate DAT and the Tn insertions may be polar, interrupting *fadD23*
159 expression and DAT synthesis (Figs. 1C, 1D, 1G). No defects in trehalose dimycolate (TDM)
160 synthesis were observed, which is transported by MmpL3[33] (Fig. 1G).
161
162 **BPs∆*33*HTH_HRM10 mutants in the predicted tail spike gene are TPP-independent**
163
164 Although BPs∆*33*HTH_HRM10 does not efficiently infect *M. abscessus* TPP synthesis mutants,
165 plaques were observed at high phage titers that are candidates for TPP-independent mutants
166 (Fig. 1E). Five individual plaques were purified, shown to have heritable infection of *M.*
167 *abscessus* TPP mutants, and were further characterized. Two were isolated on *M. abscessus*
168 GD01 *fadD23::Tn* (phKSW2 and phKSW3), two on GD01 *pE::Tn* (phKSW4 and phKSW5), and
169 one on GD180_RM2 (BPs_REM1; see below); an additional mutant (phKSW1) was isolated on
170 *M. smegmatis* ∆*MSMEG_5439* (Table S2; see below). These mutants form clear plaques on all
171 TPP synthesis pathway mutants tested (Fig. 2A), and sequencing showed that all have single
172 amino acid substitutions in the predicted BPs tail spike protein, gp22 (Table S2). Interestingly,
173 two of these substitutions, gp22 A306V and A604E (present in phKSW3 and phKSW5,
174 respectively), were reported previously as BPs host range mutants able to infect *M.*
175 *tuberculosis*[18,28]. The gp22 A604E substitution is also present in phage BPs∆*33*HTH_HRM[GD03]
176 that infects some other *M. abscessus* strains[4]. Although phKSW4 (and phKSW2; Table S2) has
177 a gp22 L462R substitution, BPs_REM1 has both a gp22 L462R substitution and a G780R
178 substitution. BPs_REM1 forms somewhat clearer plaques than phKSW4 on the TPP mutants
179 (Fig. 2A) suggesting the G780R has an additive effect towards clear plaque formation.
180

181 **TPPs are required for efficient adsorption of BPs∆*33*HTH_HRM10 to *M. abscessus* GD01**

182

183 Because TPPs are surface-exposed and are required for BPs∆*33*HTH_HRM10 infection, we
184 tested if they are required for adsorption (Fig. 2B). Wild-type BPs adsorbs relatively poorly to *M.*
185 *smegmatis*[18] and BPs∆*33*HTH_HRM10 adsorption is similarly poor on *M. abscessus* GD01 (Fig.
186 2B). However, BPs∆*33*HTH_HRM10 is clearly defective in adsorption to a GD01 *fadD23*::Tn
187 mutant (Fig. 2B, left panel). Interestingly, the TPP-independent phage phKSW1 (Table S2)
188 adsorbs considerably faster to GD01 (as does a BPs gp22 A604E mutant in *M. smegmatis*[18])
189 than its parent phage (Fig. 2B, middle panel), and shows only a small improvement in
190 adsorption on the GD01 *fadD23*::Tn mutant relative to BPs∆*33*HTH_HRM10 infection of GD01
191 (Fig. 2B). In contrast, ZoeJ∆*43-45* adsorbs similarly to both *M. abscessus* strains (Fig. 2B, right
192 panel).

193

194 **Muddy mutants in the predicted tail spike gene *24* are also TPP-independent**

195

196 We similarly isolated a resistance escape mutant of Muddy (Muddy_REM1, Table 2) and –
197 together with three Muddy mutants with expanded *M. tuberculosis*[19] host ranges – characterized
198 their infection of TPP pathway mutants (Fig. 2C). Three of the mutants (Muddy_REM1,
199 Muddy_HRM^{N0157}-1 and Muddy_HRM^{N0052}-1) efficiently infect all of the TPP pathway mutants;
200 Muddy_HRM^{N0157}-2 forms very turbid plaques on all of the mutants similar to wild-type Muddy
201 (Fig. 2C). Sequencing showed that Muddy_REM1 contains a single base substitution in the tail
202 spike gene *24* conferring a E680K substitution (Table S2), the same substitution as in
203 Muddy_HRM^{N0052}-1; Muddy_HRM^{N0157}-1 and Muddy_HRM^{N0157}-2 have G487W and T608A
204 substitutions in gp24, respectively[19].

205

206 **Spontaneous *M. abscessus* phage resistant mutants in the TPP pathway**

207

208 We previously reported *M. abscessus* mutants spontaneously resistant to BPs derivatives[9]. Two
209 of the strains (GD17_RM1 and GD22_RM4, Table S3) have mutations in *pks* and are at least
210 partially resistant to BPs∆*33*HTH_HRM10[9]. We have similarly isolated three additional
211 spontaneous mutants resistant to BPs∆*33*HTH_HRM10, two of which (GD38_RM2 and
212 GD59_RM1) have mutations in *pks*; the third (GD180_RM2) has a nonsense mutation in
213 *mmpL10* (Table S3). BPs∆*33*HTH_HRM10 does not form plaques on mutants GD38_ RM2,
214 GD17_RM1 or GD59_RM1 and very small plaques at a reduced EOP on GD22_RM4 (Fig. 3A).
215 Thus, point mutations in *M. abscessus* TPP synthesis genes can give rise to BPs resistance,
216 although these have not been observed clinically[5]. These mutants are infected well by other
217 phages we tested that infect the parent strain (Fig. 3A).

218

219 The *M. abscessus* Pks protein (MAB_0939) is a 3697-residue multidomain protein (Fig. 3B).
220 Two of the spontaneously resistant mutants have frameshift mutations close to the midpoint of
221 the gene (at codons 2,115 and 2,389, Table S3, Fig. 3B) and two others have amino acid
222 substitutions in the N-terminal Keto-synthase (KS) domain (Table S3, Fig. 3B). We note that the
223 two frameshift mutations are in the second Acyltransferase (AT) domain and leave the upstream
224 domains intact (Fig. 3B).

225

226 **Some phage-insensitive *M. abscessus* clinical isolates are naturally defective in TPPs**

227

228 *M. abscessus* clinical isolates vary greatly in their sensitivity to BPs_∆*33*HTH_HRM10 and
229 Muddy[9]. There are likely numerous determining factors, but these could include loss of TPPs.
230 Analysis of the TPP synthesis proteins (Pks, PE, PapA3, MmpL10 and FadD23) of 143

231 sequenced clinical isolates and reference strain ATCC 19977 identified 37 distinct genotypes
232 that generally correlate with global nucleotide similarity (Fig. 3C); however, no evident
233 correlation between these variations and sensitivity to BPs_Δ*33*HTH_HRM10 and/or Muddy was
234 observed (Fig. 3C). Most of the variations observed reflect amino acid substitutions, although
235 two strains (GD262 and GD273) have identical large deletions in *pks* (3,645 bp) and two others
236 (GD155 and GD286) have translocations resulting in 30.2 kbp insertions in *pks* (Fig. 3D). Both
237 GD273 and GD286 have phage infection profiles consistent with TPP loss, and the TPP-
238 independent mutant Muddy_HRM^{N0052}-1 overcomes the defect (Fig. 3E). GD262, GD273 and
239 GD286 are not susceptible to BPsΔ*33*HTH_HRM10 or the TPP-independent mutant BPs_REM1
240 (Fig. 3E), and these strains likely carry additional phage defense mechanisms targeting BPs
241 and its derivatives. GD155 has a smooth colony morphotype (Fig. 3C) and is not susceptible to
242 any of the phages tested here.
243
244 **Complementation restores TPP synthesis and phage infection**
245
246 Mutants GD22_RM4 and GD180_RM2 – defective in *pks* and *mmpL10,* respectively (Fig. 4A) –
247 can both be complemented to fully restore BPsΔ*33*HTH_HRM10 and Muddy infection (Fig. 4B).
248 Both mutants lack cell wall TPPs, and TPPs are at least partially restored by complementation
249 (Fig. 4C). Furthermore, a derivative of BPs expressing mCherry[34] – which behaves similarly to
250 BPsΔ*33*HTH_HRM10 in plaque assays (Fig. 4B) and liquid infections (Fig. 4D) – gives
251 fluorescence from parent strains, but not from GD22_RM4 and GD180_RM2 (Fig. 4E, F).
252 Complementation fully restores liquid infection of GD180_RM2, and partially restores infection
253 of GD22_RM4 (Fig. 4D), as well as fluorescence with the reporter phage (Fig. 4E, F). These
254 data are consistent with an early defect in phage infection in these mutants, consistent with loss

255 of adsorption to the cell surface. We note that disruption of TPP synthesis does not interfere
256 with Ziehl-Neelsen staining of the bacteria or alter antibiotic sensitivities (Fig. S2).
257
258 ***M. smegmatis* mutants in the TPP synthesis pathway are resistant to phages**
259 **BPs_Δ*33*HTH_HRM10 and Muddy**
260
261 *M. smegmatis* is genetically tractable and susceptible to a large number of diverse phages, and
262 using TPP mutants in *pks (MSMEG_0408)*, *mmpL10 (MSMEG_0410)*, and *pE*
263 *(MSMEG_0412)*[23,35] we showed that these have similar – albeit somewhat milder – phenotypes
264 to *M. abscessus* TPP mutants (Fig. 5A). As expected, Δ*pks,* Δ*mmpL10* and Δ*pE* mutants failed
265 to produce TPPs, whilst complementation restores the presence of TPPs (Fig. 5B). The
266 relatively efficient infection of the Δ*fadD23* mutant is consistent with incomplete TPP loss,
267 possibly due to an unidentified fatty acyl-AMP ligase partially overcoming the defect[23]. Muddy
268 similarly forms very turbid plaques on the Δ*pks* and Δ*papA3* mutants, but only mildly so on the
269 Δ*fadD23* mutant (Fig. 5A). Interestingly, the TPP-independent BPs and Muddy mutants infect *M.*
270 *smegmatis* TPP mutants normally (Fig. 5A). Complementation of the Δ*papA3*, Δ*pks*, Δ*mmpL10*,
271 and Δ*pE* mutants restores normal infection by both Muddy and BPsΔ*33*HTH_HRM10 (Fig. S3).
272
273 BPs_Δ*33*HTH_HRM10 and its mCherry derivatives are both defective in liquid infection of the
274 Δ*pks*, Δ*mmpL10*, and Δ*pE M. smegmatis* mutants, and efficient infection and lysis is restored by
275 complementation (Fig. S3A, E). The mCherry reporter phage shows fluorescence in wild-type
276 *M. smegmatis*, but loss of fluorescence in infection of all three mutants, with restoration of
277 infection in the complemented strains (Fig. S3B, C). In addition, the mCherry fluorophage
278 behaves similarly to its parent in plaque assays on *M. smegmatis* mutant and complemented
279 strains (Fig. S3E). Both BPsΔ*33*HTH_HRM10 and the TPP-independent phKSW1 are defective

280 in adsorption of a Δ*pks* mutant relative to wild type *M. smegmatis* (Fig. 5C), similar to *M.*
281 *abscessus* (Fig. 2B).
282 Testing a broader phage panel showed that most are not dependent on TPPs, with the
283 exceptions of ShedlockHolmes, MsGreen, and Papyrus, in Clusters/Subclusters K3, L3, and R,
284 respectively, which show some TPP-dependence (Fig. 5D). MsGreen and ShedlockHolmes
285 have tail genes related to Muddy gene *24*, although we note that ZoeJ does so also, and yet is
286 not TPP-dependent. However, such variation is not unexpected, as the escape mutant
287 observations show that only a single amino acid substitution is sufficient to confer TPP
288 independence (Figs. 2A, 2C, 5A).
289
290 **Resistance to BPs and Muddy TPP-independent phages reveals new resistance**
291 **mechanisms.**
292
293 The TPP-independent phage mutants infect *M. abscessus* efficiently, and we therefore repeated
294 the selection for Tn insertion mutants to explore if there are other surface molecules required for
295 infection. Interestingly, such mutants arise from the same library at a 100-fold lower abundance
296 than BPsΔ*33*HTH_HRM10 and Muddy resistant mutants (Fig. 6A, Table S1). All but one of the
297 phKSW1 resistant mutants analyzed are similarly resistant to BPsΔ*33*HTH_HRM10, BPs_REM1
298 and phKSW1 but remain sensitive to Muddy and Muddy_REM1 (Fig. 6B); One (RM10) is
299 resistant to phKSW1 but is sensitive to BPs_REM1 and is resistant to Muddy but not
300 Muddy_REM1 (Fig. 6B). One of the two Muddy_REM1 resistant mutants is only partially
301 resistant to Muddy and Muddy_REM1, but both are fully sensitive to all of the BPs derivatives
302 (Fig. 6B).
303

304 Characterization of these mutants shows that they are unlikely to be defective in surface
305 recognition by the phages. Two Muddy_REM1-resistant strains have Tn insertions in
306 transcription genes *greA* and *rpoC* (Table S1), and one phKSW1 resistant mutant maps in *recB*
307 (*MAB_0399c*; Table S1); these are unlikely to be directly involved in phage binding. Four of the
308 phKSW1-resistant mutants (RM2, RM5, RM7, and RM8), representing at least three
309 independent insertions (Fig. 6, S5) have transposons at GD01 coordinate 1,169,901, in a region
310 absent from ATCC19977 and many other *M. abscessus* strains and within a candidate 'phage-
311 inducible chromosomal island' (PICI) (Fig. 6C, Table S1). The insertions are upstream of GD01
312 gene *EXM25_05825* encoding a protein with a DUF4145 domain, which is implicated in a
313 variety of viral defense systems and is often fused with restriction endonucleases and abortive
314 infection systems[36-38] (Fig. 6C). It is plausible that the BPs resistant phenotype results from
315 overexpression of this gene.
316
317 Analysis of the cell wall lipids shows that all of the mutants retain TPPs with the exception of
318 GD01Tn_phKSW1_RM10 (Fig. 6D), which has a Tn insertion in *papA3* in addition to a
319 secondary insertion in *MAB_1686* (Table S1). Two additional mutants (GD01Tn_phKSW1_RM1
320 and RM4) have an insertion in the nearby *MAB_1690* gene and have normal TPPs (Fig. 6D);
321 *MAB_1686* and *MAB_1690* are within a large (22 kbp) operon encoding an Mce4 transport
322 system (Table S1). However, this Mce4 system is likely not acting as a receptor as the
323 Tn_phMSW1_RM1 mutant does not have an adsorption defect (Fig. 6E). The
324 Tn_phKSW1_RM2 mutant also does not have any adsorption defect (Fig. 6E).
325
326 **Discussion**
327
328 Trehalose polyphleates are among the largest known lipids in mycobacteria and are structurally
329 related to sulfolipids SL-1 and polyacylated trehalose PAT, which in contrast to TPPs, are found

330 exclusively in *M. tuberculosis*. The roles of TPPs in mycobacterial physiology and/or growth
331 remain unclear, but are implicated in clumping and cording in *M. abscessus*[24]. Many TPP-
332 defective *M. abscessus* strains have rough morphotypes – typically associated with cording –
333 consistent with the rough colony morphology primarily resulting from GPL loss[22]. Clearly, TPPs
334 are critical for adsorption of several phages, including the therapeutically useful Muddy and
335 BPs[4,5]. The finding that both phages require TPPs is a surprise, as they are genomically distinct,
336 share few genes, and were thus considered to be suitable for combination in phage cocktails.
337 Nonetheless, the availability of TPP-independent phage mutants provides substitutes to which
338 resistance both occurs at a much lower frequency, and such mutants do not typically show co-
339 resistance to the two phages. We propose that the TPP-independent phage replace their
340 cognate parent phages in therapeutic cocktails.
341
342 A simple explanation for the role of TPPs is that they are specifically recognized and bound to
343 by BPs, Muddy and the other TPP-dependent phages as the only requirement for DNA injection.
344 However, it is then unclear as to how the TPP-independent phages overcome TPP loss, and it
345 seems implausible that they gain the ability to bind to a completely different receptor. A more
346 likely explanation is that TPPs act as co-receptors for Muddy and BPs and facilitate recognition
347 of a different surface molecule; the TPP-independent phage mutants would then simply bypass
348 the need for activation by TPPs. The observation that tail spike mutants such as phKSW1
349 adsorb substantially better than the parent phage, even to TPP-containing host cells, is
350 consistent with this latter explanation. Furthermore, wild-type BPs does not efficiently infect *M.*
351 *tuberculosis* H37Rv, but a mutant with the gp22 A604E substitution enables efficient infection[18],
352 even though *M. tuberculosis* lacks TPPs[39]. Similarly, wild-type Muddy efficiently infects *M.*
353 *tuberculosis* H37Rv[19] despite its lack of TPPs, and Muddy tail spike substitutions expand its
354 host range to other *M. tuberculosis* strains[19]. These observations not only suggest that TPPs
355 are not the receptors *per se* for these phages, but that there may be general mechanisms

356 governing receptor access by the phages, together with phage strategies for expanding host cell
357 recognition and infection. Furthermore, if TPPs are not the target of direct phage recognition,
358 the true receptor is likely to be encoded by genes that are essential for mycobacterial viability.
359 Thus, although transposon insertion mutagenesis has been used in other systems for identifying
360 phage receptors[40-43], this maybe of more limited use in *Mycobacterium*, although as we have
361 shown here, it is useful for mapping a plethora of resistance mechanisms.
362
363 Understanding the roles of TPPs in *M. abscessus* is important for therapeutic phage use, and
364 we note that in at least some clinical isolates the loss of TPPs through gene deletions or
365 translocation leads to loss of infection by BPs∆*33*HTH_HRM10 or Muddy. In the first therapeutic
366 use of mycobacteriophages, BPs∆*33*HTH_HRM10 and Muddy were used in combination with
367 ZoeJ, and it is of interest that ZoeJ is not TPP-dependent. We also note that resistance to BPs
368 derivatives or Muddy has not been observed in clinical use, even in 11 cases where only a
369 single phage was used[5]. It is plausible that resistance through TPP loss has a tradeoff with
370 fitness, and the roles of TPPs in *M. abscessus* pathogenicity warrant further study.
371
372 Finally, transposon mutagenesis and selection of mutants resistant to the TPP-independent
373 phages reveals additional mechanisms of phage resistance. Particularly intriguing is the
374 isolation of insertions in a candidate PICI, with the potential to activate expression of a PICI
375 gene implicated in phage defense. These *Mycobacterium* PICIs and their roles in phage
376 infection profiles deserve further investigation.
377
378 **Acknowledgements**
379 We thank Chidiebere Akusobi, Mark Sullivan, Kerry McGowen, Carlos Rodriguez and William
380 DePas for helpful discussions. We also thank all of the students and faculty in the SEA-

381 PHAGES program that discovered and characterized phages used in this study, and the
382 numerous colleagues that provided *M. abscessus* strains in the GDxx series. Microscopy and
383 flow cytometry were performed at the Montpellier Imaging Center for Microscopy (MRI). This
384 work was supported by grants from the National Institutes of Health grants GM131729 and the
385 Howard Hughes Medical Institute Grant GT12053 to GFH, a Cystic Fibrosis Foundation Postdoc
386 Fellowship WETZEL21F0 to KSW, by the French National Research Agency ANR-21-CE44-
387 0027-01 (MYCOLT) to LK and CC and by Vaincre la Mucoviscidose (RF20200502678) and the
388 Association Grégory Lemarchal for funding the PhD fellowship of MI.
389

390 **Declaration of interests**

391

392 GFH receives support through a Collaborative Research Agreement with Janssen Inc., but
393 which did not fund the work reported here.

394 **Materials and Methods**

395 **Bacterial strains and culture conditions**

396 Bacterial strains (Table S4) were grown in Middlebrook 7H9 media (BD Difco) supplemented
397 10% oleic acid, albumin, dextrose, catalase (OADC enrichment) (7H9/OADC) or on Middlebrook
398 7H10/OADC solid media (BD Difco) at 37° C. Antibiotics were added when required.
399 Transformations of electrocompetent mycobacteria were performed using a Bio-Rad Gene
400 pulser (25 µF, 2500 V, 800 Ohms). For some *M. smegmatis* strains, Tween-80 (0.05%) was
401 used in starter cultures but omitted in subcultures used for phage infections. Cultures used in
402 phage infection were supplemented with 1 mM $CaCl_2$. When required, *M. abscessus* strains
403 were selected with 1 mg/mL hygromycin or 200 µg/mL streptomycin, and *M. smegmatis* were
404 selected with 50 µg/mL hygromycin. *M. abscessus* strains in the GDxx series are part of the
405 strain collection at the University of Pittsburgh and were kindly provided by numerous
406 colleagues.

407

408 **Engineering of MycoMarT7-Hyg2**

409 Phage MycoMarT7-Hyg1 and MycoMarT7-Hyg2 were engineered from phage MycoMarT7
410 using CRISPY-BRED recombineering[30]. Briefly, dsDNA recombineering substrates were
411 designed that contained the desired mutation (a HygR cassette) with flanking sequences to
412 permit the replacement of either KanR (MycoMarT7-Hyg1) or KanR and oriR6K (MycoMarT7-
413 Hyg2). These substrates and genomic DNA from MycoMarT7 were transformed into *M.*
414 *smegmatis* mc^2155 recombineering cells that contain the plasmid pJV138[30]. Transformations
415 were combined with cells containing a CRISPR plasmid selecting against the parent
416 MycoMarT7 and plated on solid media; this enriches for mutants containing the allelic
417 replacement that form plaques on the plate. Resulting plaques were screened for presence of
418 the Hyg-marked transposon by PCR, and positive plaques were plaque purified, whole genome
419 sequenced, and confirmed to have retained temperature sensitivity.

420

421 **Construction of the *M. abscessus* GD01 transposon insertion library and phage**

422 **challenge**

423 The transposon mutagenesis library was largely prepared as previously described[31]. Briefly, 50

424 mL of *M. abscessus* GD01 was grown to an OD_{600} of 0.2. The cells were pelleted and

425 resuspended in 1 mL of phage buffer (10 mM Tris HCl, pH 7.5; 10 mM $MgSO_4$; 68.5 mM NaCl; 1

426 mM $CaCl_2$), pre-warmed to 37° C and infected with 800 µL MycoMarT7-Hyg2 ($5x10^{10}$ pfu/mL).

427 The cells and MycoMarT7-Hyg2 were incubated at 37° C for 7.5 hours. Cells were pelleted and

428 resuspended in 8 mL PBS + 0.05% Tween80, and the resuspension was combined with 8 mL

429 40% glycerol for freezing at -80° C. The transduction frequency was determined by measuring

430 hygromycin resistant colonies/mL and 120,000 transductants were plated onto large square

431 plates containing solid 7H10/OADC media with 0.1% Tween80 and 1 mg/mL hygromycin. Plates

432 incubated at 37° C for nine days. To harvest the library, cells were scraped off the solid media,

433 resuspended in 7H9/OADC combined with 40% glycerol, aliquoted and frozen at -80° C.

434

435 To identify GD01 insertion mutants that were resistant to phage infection, ~20 µL of GD01 Tn

436 library was thawed and grown overnight to an OD_{600} of 0.175. Dilutions of this culture

437 (approximately 10^4, 10^5 and 10^6 cells) were spread onto 7H10/OADC solid media plates seeded

438 with or without 10^8 pfu of phages BPs_Δ*33*HTH_HRM10, Muddy phKSW1 or Muddy_REM1.

439 Plates were incubated at 37° C for seven days. Colonies able to grow on phage-seeded plates

440 were subjected to PCR to identify a transposon insertion site (see below) and struck out two

441 times to remove any remaining phage. After streaking, single colonies were grown in liquid

442 media and used for phage susceptibility testing by standard plaque assay.

443

444 **Identification of transposon insertion sites**

445 Transposon insertion sites were identified by PCR using a primer that annealed to the
446 transposon in the hygromycin resistance gene (Tn_Hyg_Fwd_2: 5'-
447 CTTCACCTTCCTGCACGACT-3'), and a primer with a degenerate 3' end, or if that did not yield
448 an amplicon, nested PCR with primers Tn_Hyg_Fwd_2 and Primer 557 (5'-
449 GGCCAGCGAGCTAACGAGCANNNNNNNGTT-3') followed by PCR with primers Primer 414
450 (5'-GGCCAGCGAGCTAACGAGAC-3') and Tn_Hyg_Fwd_1 (5'-
451 TTCGAGGTGTTCGAGGAGAC-3'). Amplicons were gel extracted, Sanger sequenced from the
452 transposon, and the result aligned to the GD01 sequence to identify the transposon insertion
453 site. For most strains (and at least one strain per interrupted gene), the transposon insertion site
454 was confirmed by designing primers that flanked the site identified by the initial PCR and
455 confirming that this region had increased in size by 1,259 bp compared to strain GD01.
456
457 **Screening of phage susceptibility**
458 Phage susceptibility profiles were assessed using standard plaque assays. Top agar bacterial
459 lawns were made by combining Middlebrook Top Agar (MBTA; Middlebrook 7H9, 1 mM $CaCl_2$,
460 0.35% BactoAgar) with 300 µL-500 µL cell culture. After top agar had solidified, phages were
461 10-fold serially diluted and spotted onto the top agar bacterial lawns and incubated 24-48 hours
462 (*M. smegmatis*) or 5-7 days (*M. abscessus*) until bacterial lawns were confluent. Phages used
463 in this study were obtained from University of Pittsburgh and *M. smegmatis* mc^2155 was used to
464 propagate them.
465
466 **Plasmid construction**
467 To create plasmid pKSW131, *fadD23*, *pE*, *mmpL10* and *papA3* and the flanking intergenic
468 sequence was amplified using Q5 HiFi 2× MasterMix (NEB) from genomic DNA isolated from *M.*
469 *abscessus* GD01. The amplicon was purified and cloned into EcoRI-digested vector pLA155
470 using the NEBuilder Gibson Assembly Master Mix and transformed into *E. coli* strain DH5a;

471 plasmids and primers are shown in Table S5. The culture that yielded a successfully
472 constructed plasmid was grown at 30° C rather than 37° C, although it is unknown if this
473 contributed to successful plasmid maintenance in the culture. To create plasmid pKSW134, the
474 open reading frame of *fadD23* was amplified from GD01 gDNA and cloned into Pml I-digested
475 anhydrotetracycline (ATc) inducible vector pCCK39[44] using the NEBuilder Gibson Assembly
476 Master Mix. The entire plasmids were sequenced by Plasmidsaurus Inc
477 (https://www.plasmidsaurus.com/).
478
479 pMV*pks_mWasabi* and pMV*mmpL10_mWasabi* were constructed based on pMV*pks* and
480 pMV*mmpL10* by in-fusion cloning. The *mWasabi* sequence under the control of the constitutive
481 *Pleft** promoter[45] was amplified by PCR using a Q5 high-fidelity DNA polymerase (New England
482 Biolabs). Plasmids were linearized with KpnI-HF (New England Biolabs). Agarose gels were
483 used to purify linear fragments, then circularized using In-Fusion SNAP Assembly Master Mix
484 (Takara Inc.), according to the manufacturer's instructions. Stellar competent cells were used for
485 transformation. Plasmids generated were verified by sequencing.
486
487 **Isolation and whole genome sequencing of phage resistant mycobacteria mutants**
488 Two of these phage resistant mutants (GD17_RM1 and GD22 RM_4) were described
489 previously[9]; the others were isolated in the same manner. Briefly, 10^8 CFU *M. abscessus* were
490 incubated with 10^9 PFU of phage. Infections were plated on solid media at two and five days-
491 post infection, and survivors were purified, tested for phage resistance, and sequenced. The
492 mutants were sequenced as described previously[9].
493
494 **Isolation of BPs_Δ*33*HTH_HRM10 mutants**
495 Clear plaques were observed within high titer spots for phage BPs_Δ*33*HTH_HRM10 on strains
496 GD01Tn_BPs_HRM10_RM6, GD01Tn_BPs_HRM10_RM11 and GD180_RM2. These plaques

497 were picked and plated on the resistant strain two additional times to purify. A purified plaque
498 was then used to produce a high-titer phage lysate on *M. smegmatis* mc^{2}155, and subsequently
499 subjected to gene *22* PCR sequencing or whole-genome sequencing.
500
501 **Total lipids extraction of mycobacteria and TLC analysis**
502 Bacteria were grown in LB medium at 37° C without agitation and pelleted by centrifugation
503 (3,000 *g*, 10 min, room temperature). Lipids were extracted as described previously[23]. Briefly,
504 bacterial pellets were treated successively with $CHCl_3/CH_3OH$ (1:2) and $CHCl_3/CH_3OH$ (2:1),
505 washed with water and dried. Lipids were resuspended in $CHCl_3$ prior to spot on TLC. For TLC
506 analysis, silica gel G60 plates (10 x 20 cm, Macherey-Nagel) were used to spot samples and
507 lipids were separated with $CHCl_3/CH_3OH$ (90:10, v/v). Lipid profiles were shown by spraying the
508 plates with a 0.2% anthrone solution (w/v) in concentrated H_2SO_4 and charring.
509
510 **Adsorption Assays**
511 *M. smegmatis* strains were grown to an OD_{600} of 0.5-0.8, then concentrated approximately
512 tenfold to 1.75×10^9/mL. One milliliter of cells (*M. smegmatis* mc^{2}155 or mc^{2}155 Δ*pks*) were
513 infected in triplicate in a 12-well plate at a multiplicity of infection (MOI) of 0.001. At each
514 timepoint, 50 µL of liquid were removed, pelleted, and the supernatant that contained unbound
515 phage was titered on *M. smegmatis*. For *M. abscessus* GD01 and *M. abscessus* GD01
516 *fadD23*::Tn, the same protocol was followed but the strains were grown to an OD_{600} of 0.15-0.25
517 and cells were concentrated approximately tenfold to 6.3×10^8/mL.
518
519 **Growth curves of mycobacteria incubated with phages**
520 Bacterial growth assays were performed in 96-well plates (Falcon), each well containing 100 µL
521 of bacterial culture and 100 µL of phage lysates or medium as control. Exponential phage
522 cultures of mycobacteria were used and set at 3×10^7 CFU/mL in Middlebrook 7H9/OADC

523 supplemented with 1 mM $CaCl_2$. Phages were incubated at a MOI 10 and diluted in 7H9/OADC
524 supplemented with 1 mM $CaCl_2$. Measurements were taken every three hours for *M. smegmatis*
525 strains and six hours for *M. abscessus* strains using a spectrophotometer (Tecan, infinite 200
526 PRO) until stationary phase was reached (2 days for *M. smegmatis* strains and 6 days for *M.*
527 *abscessus* strains). Plates were incubated at 37° C without agitation.
528

529 **Microscopy and flow cytometry sample preparation**

530 Mycobacteria were sub-cultured in 7H9/OADC with agitation to obtain exponential phase
531 cultures. Bacteria were concentrated to obtain a sample containing $1.2x10^7$ CFU (for
532 microscopy) or $6x10^6$ CFU (for flow cytometry) and then incubated with either medium or phage
533 BPs_Δ*33*HTH_HRM10 (MOI 10) as controls or phage BPs_Δ*33*HTH_HRM10 mCherry (MOI
534 10). For *M. smegmatis* strains, the infections were performed for two hours and four hours for
535 *M. smegmatis* and *M. abscessus*, respectively, at 37° C without agitation. After infection,
536 samples were fixed with PFA 4% for 20 min at room temperature. Samples were then diluted as
537 necessary depending on the experiment with 7H9/OADC supplemented with 0.025% tyloxapol
538 and sonicated to disrupt bacterial aggregates. For microscopy, samples were then mounted
539 between coverslips and slides with Immu-Mount (Epredia). Samples were kept at 4° C in the
540 dark until analysis.
541

542 **Microscopy**

543 DIC (Differential interference contrast) and epifluorescence images were acquired on a ZEISS
544 Axio Imager Z1 up-right microscope. A 63X Plan Apochromat 1.4 NA oil objective and a 100X
545 Plan Apochromat 1.4 NA oil objective was used respectively for *M. smegmatis* or *M. abscessus*
546 strains. mCherry was excited with an Intenslight fiber lamp with Texas Red (Ex: 560/40, dic.
547 585, Em: 630/75) filter cube. Images were acquired with a scMOS ZYLA 4.2 MP.
548

549 **Image analysis**

550 Representative fields without technical artefacts were chosen. Fiji software was used to adjust
551 intensity, brightness and contrast (identically for compared image sets).

552

553 **Flow cytometry**

554 Infected bacteria were analysed by flow cytometry using a NovoCyte ACEA flow cytometer
555 (excitation laser wavelength: 561 nm, emission filter: 615/20 nm). Gates were drawn using SSC-
556 A/FSC-A and multiple cells were excluded with SSC-H / SSC-A. Uninfected cells and bacteria
557 infected by non-fluorescent phage were included as controls. Experiments were performed at
558 least twice with similar results. Approximately 300,000 events were recorded per experiment.
559 Analysis was done with NovoExpress.

560

561 **Ziehl-Nilseen staining**

562 Concentrated cultures were fixed on glass slides by heating at 150°C for 15 min followed by
563 chemical fixation with methanol. BD Carbolfuchsin kit was used following manufacturer
564 recommendations. Samples were observed using an Evos M7000 Imaging System.

565

566 **Drug susceptibility testing**

567 The CLSI guidelines[46] were followed to determine the minimum inhibitory concentrations
568 (MICs). Briefly, all cultures were incubated in Cation-adjusted Mueller-Hinton Broth (CaMHB) at
569 30°C prior experiments. Each well of a 96-well plate was filled with 100 µL of bacterial
570 suspension previously inoculated with 5.10^6 CFU/mL, except for the first column, to which 198
571 µL of the bacterial suspension was added. 2 µL of drug at its highest concentration was added
572 to the first column containing 198 µL of bacterial suspension and was two-fold serially diluted.
573 Results are obtained after 4 days of incubation at 30°C without agitation. Three independent
574 experiments were carried out in duplicate.

575

576 **Statistical analysis**

577 Statistical analysis was carried out with GraphPad Prism version 9.0.0 for Windows (GraphPad
578 Software, San Diego, California, United States). Descriptive statistics are cited and represented
579 as median and interquartile range for each of the variables calculated. A non-parametric Dunn's
580 test was used to compare the different conditions at 48 hours for *M. smegmatis* or 144 hours for
581 *M. abscessus*. A significance level *a priori* was set at $\alpha = 0.05$.

582

583 **Phylogenetic analysis of TPP pathway amino acid sequences in *M. abscessus***

584 A phylogenetic tree was constructed of a concatenated alignment of amino acid sequences of
585 the five TPP synthesis pathway members for 143 clinical isolates of *M. abscessus* and *M.*
586 *abscessus* ATCC19977. Homologs were identified using MMSeqs2 and phammseqs[47] and
587 subsequently aligned using ClustalO and Trimal[48]. A concatenated alignment was generated
588 with a custom python script and the maximum likelihood phylogeny was generated using
589 RAxML[49].

590

591 **References**

592 1. Martiniano, S.L., Nick, J.A. & Daley, C.L. Nontuberculous Mycobacterial Infections in Cystic
593 Fibrosis. *Thorac Surg Clin* **29**, 95-108 (2019).
594 2. Johansen, M.D., Herrmann, J.L. & Kremer, L. Non-tuberculous mycobacteria and the rise of
595 Mycobacterium abscessus. *Nat Rev Microbiol* **18**, 392-407 (2020).
596 3. Nick, J.A., Daley, C.L., Lenhart-Pendergrass, P.M. & Davidson, R.M. Nontuberculous
597 mycobacteria in cystic fibrosis. *Curr Opin Pulm Med* **27**, 586-592 (2021).
598 4. Dedrick, R.*, et al.* Engineered bacteriophages for treatment of a patient with a disseminated
599 drug-resistant *Mycobacterium abscessus*. *Nature Medicine* **25**, 730-733 (2019).
600 5. Dedrick, R.M.*, et al.* Phage Therapy of Mycobacterium Infections: Compassionate-use of
601 Phages in Twenty Patients with Drug-Resistant Mycobacterial Disease. *Clin Infect Dis*,
602 ciac453 (2022).
603 6. Nick, J.A.*, et al.* Host and pathogen response to bacteriophage engineered against
604 Mycobacterium abscessus lung infection. *Cell* **185**, 1860-1874 e1812 (2022).
605 7. Little, J.S.*, et al.* Bacteriophage treatment of disseminated cutaneous Mycobacterium
606 chelonae infection. *Nat Commun* **13**, 2313 (2022).
607 8. Hatfull, G.F. Mycobacteriophages: From Petri dish to patient. *PLoS Pathog* **18**, e1010602
608 (2022).
609 9. Dedrick, R.M.*, et al.* Mycobacterium abscessus Strain Morphotype Determines Phage
610 Susceptibility, the Repertoire of Therapeutically Useful Phages, and Phage Resistance.
611 *mBio* **12**(2021).
612 10. Hatfull, G.F., Dedrick, R.M. & Schooley, R.T. Phage Therapy for Antibiotic-Resistant
613 Bacterial Infections. *Annu Rev Med* **73**, 197-211 (2022).
614 11. Hatfull, G.F. Actinobacteriophages: Genomics, Dynamics, and Applications. *Annu Rev Virol*
615 **7**, 37-61 (2020).

616 12. Chen, J.*, et al.* Defects in glycopeptidolipid biosynthesis confer phage I3 resistance in
617 Mycobacterium smegmatis. *Microbiology* **155**, 4050-4057 (2009).
618 13. Russell, D.A. & Hatfull, G.F. PhagesDB: the actinobacteriophage database. *Bioinformatics*
619 **33**, 784-786 (2017).
620 14. Pedulla, M.L.*, et al.* Origins of highly mosaic mycobacteriophage genomes. *Cell* **113**, 171-
621 182 (2003).
622 15. Pope, W.H.*, et al.* Whole genome comparison of a large collection of mycobacteriophages
623 reveals a continuum of phage genetic diversity. *Elife* **4**, e06416 (2015).
624 16. Hatfull, G.F.*, et al.* Comparative Genomic Analysis of 60 Mycobacteriophage Genomes:
625 Genome Clustering, Gene Acquisition, and Gene Size. *J Mol Biol* **397**, 119-143 (2010).
626 17. Hatfull, G.F.*, et al.* Exploring the mycobacteriophage metaproteome: phage genomics as an
627 educational platform. *PLoS Genet* **2**, e92 (2006).
628 18. Jacobs-Sera, D.*, et al.* On the nature of mycobacteriophage diversity and host preference.
629 *Virology* **434**, 187-201 (2012).
630 19. Guerrero-Bustamante, C.A., Dedrick, R.M., Garlena, R.A., Russell, D.A. & Hatfull, G.F.
631 Toward a Phage Cocktail for Tuberculosis: Susceptibility and Tuberculocidal Action of
632 Mycobacteriophages against Diverse Mycobacterium tuberculosis Strains. *mBio* **12**(2021).
633 20. Abrahams, K.A. & Besra, G.S. Synthesis and recycling of the mycobacterial cell envelope.
634 *Curr Opin Microbiol* **60**, 58-65 (2021).
635 21. Gutierrez, A.V., Viljoen, A., Ghigo, E., Herrmann, J.L. & Kremer, L. Glycopeptidolipids, a
636 Double-Edged Sword of the Mycobacterium abscessus Complex. *Front Microbiol* **9**, 1145
637 (2018).
638 22. Bernut, A.*, et al.* Insights into the smooth-to-rough transitioning in Mycobacterium bolletii
639 unravels a functional Tyr residue conserved in all mycobacterial MmpL family members.
640 *Mol Microbiol* **99**, 866-883 (2016).

641 23. Burbaud, S., *et al.* Trehalose Polyphleates Are Produced by a Glycolipid Biosynthetic
642 Pathway Conserved across Phylogenetically Distant Mycobacteria. *Cell Chem Biol* **23**, 278-
643 289 (2016).
644 24. Llorens-Fons, M., *et al.* Trehalose Polyphleates, External Cell Wall Lipids in Mycobacterium
645 abscessus, Are Associated with the Formation of Clumps with Cording Morphology, Which
646 Have Been Associated with Virulence. *Front Microbiol* **8**, 1402 (2017).
647 25. Thouvenel, L., *et al.* The final assembly of trehalose polyphleates takes place within the
648 outer layer of the mycobacterial cell envelope. *J Biol Chem* **295**, 11184-11194 (2020).
649 26. Hatfull, G.F. Phage Therapy for Nontuberculous Mycobacteria: Challenges and
650 Opportunities. *Pulm Ther* **9**, 91-107 (2023).
651 27. Dedrick, R.M., *et al.* Mycobacteriophage ZoeJ: A broad host-range close relative of
652 mycobacteriophage TM4. *Tuberculosis (Edinb)* **115**, 14-23 (2019).
653 28. Sampson, T., *et al.* Mycobacteriophages BPs, Angel and Halo: comparative genomics
654 reveals a novel class of ultra-small mobile genetic elements. *Microbiology* **155**, 2962-2977
655 (2009).
656 29. Johansen, M.D., *et al.* Mycobacteriophage-antibiotic therapy promotes enhanced clearance
657 of drug-resistant Mycobacterium abscessus. *Dis Model Mech* **14**(2021).
658 30. Wetzel, K.S., *et al.* CRISPY-BRED and CRISPY-BRIP: efficient bacteriophage engineering.
659 *Sci Rep* **11**, 6796 (2021).
660 31. Akusobi, C., *et al.* Transposon mutagenesis in Mycobacterium abscessus identifies an
661 essential penicillin-binding protein involved in septal peptidoglycan synthesis and antibiotic
662 sensitivity. *Elife* **11**(2022).
663 32. Rifat, D., Chen, L., Kreiswirth, B.N. & Nuermberger, E.L. Genome-Wide Essentiality
664 Analysis of Mycobacterium abscessus by Saturated Transposon Mutagenesis and Deep
665 Sequencing. *mBio* **12**, e0104921 (2021).

666 33. Grzegorzewicz, A.E., *et al.* Inhibition of mycolic acid transport across the Mycobacterium
667 tuberculosis plasma membrane. *Nat Chem Biol* **8**, 334-341 (2012).
668 34. Dulberger, C.L., *et al.* Mycobacterial nucleoid-associated protein Lsr2 is required for
669 productive mycobacteriophage infection. *Nat Microbiol* (2023).
670 35. Judd, J.A., *et al.* A Mycobacterial Systems Resource for the Research Community. *mBio*
671 **12**(2021).
672 36. Vassallo, C.N., Doering, C.R., Littlehale, M.L., Teodoro, G.I.C. & Laub, M.T. A functional
673 selection reveals previously undetected anti-phage defence systems in the E. coli
674 pangenome. *Nat Microbiol* **7**, 1568-1579 (2022).
675 37. Anantharaman, V., Makarova, K.S., Burroughs, A.M., Koonin, E.V. & Aravind, L.
676 Comprehensive analysis of the HEPN superfamily: identification of novel roles in intra-
677 genomic conflicts, defense, pathogenesis and RNA processing. *Biol Direct* **8**, 15 (2013).
678 38. Makarova, K.S., Wolf, Y.I. & Koonin, E.V. Comparative genomics of defense systems in
679 archaea and bacteria. *Nucleic Acids Res* **41**, 4360-4377 (2013).
680 39. Touchette, M.H., *et al.* The rv1184c locus encodes Chp2, an acyltransferase in
681 Mycobacterium tuberculosis polyacyltrehalose lipid biosynthesis. *J Bacteriol* **197**, 201-210
682 (2015).
683 40. McKitterick, A.C. & Bernhardt, T.G. Phage resistance profiling identifies new genes required
684 for biogenesis and modification of the corynebacterial cell envelope. *Elife* **11**(2022).
685 41. Bohm, K., *et al.* Genes affecting progression of bacteriophage P22 infection in Salmonella
686 identified by transposon and single gene deletion screens. *Mol Microbiol* **108**, 288-305
687 (2018).
688 42. Mutalik, V.K., *et al.* High-throughput mapping of the phage resistance landscape in E. coli.
689 *PLoS Biol* **18**, e3000877 (2020).

690 43. Kortright, K.E., Chan, B.K. & Turner, P.E. High-throughput discovery of phage receptors
691 using transposon insertion sequencing of bacteria. *Proc Natl Acad Sci U S A* **117**, 18670-
692 18679 (2020).
693 44. Ko, C.C. & Hatfull, G.F. Mycobacteriophage Fruitloop gp52 inactivates Wag31 (DivIVA) to
694 prevent heterotypic superinfection. *Mol Microbiol* **108**, 443-460 (2018).
695 45. Nesbit, C.E., Levin, M.E., Donnelly-Wu, M.K. & Hatfull, G.F. Transcriptional regulation of
696 repressor synthesis in mycobacteriophage L5. *Mol Microbiol* **17**, 1045-1056 (1995).
697 46. Woods, G.L.*, et al.* Susceptibility testing of mycobacteria, nocardiae and other aerobic
698 actinomycetes. in *Susceptibility Testing of Mycobacteria, Nocardiae, and Other Aerobic*
699 *Actinomycetes* (Wayne (PA), 2011).
700 47. Gauthier, C.H., Cresawn, S.G. & Hatfull, G.F. PhaMMseqs: a new pipeline for constructing
701 phage gene phamilies using MMseqs2. *G3 (Bethesda)* **12**(2022).
702 48. Capella-Gutierrez, S., Silla-Martinez, J.M. & Gabaldon, T. trimAl: a tool for automated
703 alignment trimming in large-scale phylogenetic analyses. *Bioinformatics* **25**, 1972-1973
704 (2009).
705 49. Stamatakis, A., Ludwig, T. & Meier, H. RAxML-III: a fast program for maximum likelihood-
706 based inference of large phylogenetic trees. *Bioinformatics* **21**, 456-463 (2005).
707 50. Bachmann, B.O. & Ravel, J. Chapter 8. Methods for in silico prediction of microbial
708 polyketide and nonribosomal peptide biosynthetic pathways from DNA sequence data.
709 *Methods Enzymol* **458**, 181-217 (2009).
710

711 **Figure Legends**

712

713 **Figure 1. Identification of phage-resistant transposon insertion mutants of *M. abscessus***
714 **GD01**. **A**. Construction of MycoMarT7-Hyg1 and MycoMarT7-Hyg2. Transposon delivery phage
715 phiMycoMarT7 delivers a transposon containing *Escherichia coli* ori6Kγ (grey) and kanamycin
716 resistance cassette (blue), flanked by inverted repeats (yellow boxes). CRISPY-BRED[30] was
717 used to create phiMycoMarT7-Hyg1 and phiMycoMarT7-Hyg2, which deliver transposons
718 containing oriR6K (grey box) and a hygromycin resistance cassette (red box), or only a
719 hygromycin resistance cassette. **B**. *M. abscessus* GD01 or a transposon library of *M. abscessus*
720 strain GD01 (*M.ab* GD01 Tn Lib) were plated on solid media or solid media seeded with phage
721 BPs_Δ*33*HTH_HRM10 (or Muddy; not shown). **C**. Locations of transposon insertions in the TPP
722 locus in phage resistant mutants. Red and black bars show the locations of insertion isolated as
723 resistant to BPs_Δ*33*HTH_HRM10 and Muddy, respectively. **D**. Proposed roles of Pks, PapA3,
724 FadD23, MmpL10 and PE in the synthesis and transport of TPPs and DAT. **E**. Tenfold serial
725 dilutions of phages were spotted onto solid media with *M. smegmatis* mc^2155, *M. abscessus*
726 GD01, or representative *M. abscessus* GD01 transposon insertion mutant strains:
727 GD01Tn_BPs_HRM10_RM1 (B_RM1); GD01Tn_BPs_HRM10_RM6 (B_RM6);
728 GD01Tn_BPs_HRM10_RM11 (B_RM11); GD01Tn_BPs_HRM10_RM10 (B_RM 10);
729 GD01Tn_BPs_HRM10_RM5 (B_RM 5). The locations of Tn insertions are indicated in
730 parentheses. Phages used are: BPs_Δ*33*HTH_HRM10 ("BPs"), Muddy, ZoeJΔ*43-45* ("ZoeJ"),
731 Itos, and Faith1Δ*38-40* ("Faith1"). Plaque assays were performed at least twice with similar
732 results. **F**. Tenfold serial dilutions of phages were spotted onto solid media with strain GD01
733 *fadD23*::Tn (GD01Tn_BPs_HRM10_RM1) containing plasmid pKSW134 with gene *fadD23*
734 under expression of an anhydrotetracycline (ATc)-inducible promoter. FadD23 is not expressed
735 in the absence of ATc (left panel) but is induced by ATc (right panel). Plaque assays were

736 performed at least twice with similar results. **G**. TLC analysis of total lipids extracted from *M.*
737 *abscessus* GD01 and mutants with transposon insertions in the TPP synthesis and transport
738 genes. *M. smegmatis* mc^{2}155 and a Δ*mmpL10* mutant strain of *M. smegmatis* are also included
739 as controls.
740
741 **Figure 2. Mutants of BPs_Δ*33*HTH_HRM10 and Muddy overcome TPP loss. A**. Ten-fold
742 serial dilutions of BPs_Δ*33*HTH_HRM10 and gp22 mutants (as indicated on left; see Table S2)
743 were spotted onto solid media with *M. smegmatis* mc^{2}155, *M. abscessus* GD01, or *M.*
744 *abscessus* GD01 transposon insertion mutant strains. Plaque assays were performed at least
745 twice with similar results. The locations of amino acid substitutions in BPs_Δ*33*HTH_HRM10
746 gp22 conferring the ability to infect TPP-deficient strains (red) or were previously found to
747 broaden host range to include *M. tuberculosis* (purple) (bottom panel). The A306V and A604E
748 substitutions were identified with both assays. **B**. Adsorption of phages BPs_Δ*33*HTH_HRM10,
749 phKSW1 and ZoeJΔ*43-45* to *M. abscessus* strains GD01 and GD01 *fadD23*::Tn
750 (GD01Tn_BPs_HRM10_RM1) as indicated by the percentage of unadsorbed phages remaining
751 in infection supernatants at different times after infection. Assays were performed in duplicate
752 twice and the mean is displayed; error bars represent one standard deviation. **C**. Tenfold serial
753 dilutions of Muddy and Muddy gp24 mutants (as indicated on left) were spotted onto solid media
754 with *M. smegmatis* mc^{2}155, *M. abscessus* GD01, or *M. abscessus* GD01 transposon insertion
755 mutant strains. Plaque assays were performed at least twice with similar results. The location of
756 amino acid substitutions in Muddy gp24 that confer the ability to infect TPP deficient strains
757 (bottom panel).
758
759 **Figure 3. Phage infection profiles of *M. abscessus* phage resistant mutants**. Tenfold serial
760 dilutions of phage lysates (as indicated on left) were spotted onto solid media with *M.*
761 *smegmatis* mc^{2}155, the parent *M. abscessus* strains or spontaneously isolated phage resistant

762 mutant (RM) derivatives. Plaque assays were performed at least twice with similar results. **B**. A
763 schematic representation of *M. abscessus* Pks showing the location of predicted functional
764 domains and the amino acid changes in spontaneous phage resistant mutants below. Domain
765 abbreviations are: AT, Acyltransferase; KS, Ketosynthase, KR, Ketoreductase; DH,
766 Dehydratase; ER, Enoylreductase; PP, phosphopantetheinylate acyl carrier protein. Domains
767 were identified using the PKS analysis web site at http://nrps.igs.umaryland.edu/ [50]. **C**. Amino
768 acid sequences from the five TPP synthesis pathway genes in 143 *M. abscessus* clinical
769 isolates (and *M. abscessus* ATCC19977) were concatenated and used to construct a
770 phylogenetic tree. Strain morphotypes are labeled as either rough (R) or smooth
771 (S). Susceptibilities to phages BPs_Δ*33*HTH_HRM10 and Muddy are represented in green and
772 red, respectively[9]. Arrows indicate strains in panels D and E. **D**. Position of large deletions
773 (GD262 and GD273) or insertions (GD155 and GD286) in the *pks* gene with respect to the
774 GD01 TPP locus. **E**. Ten-fold serial dilutions of phage lysates (as indicated on left) were spotted
775 onto solid media with either *M. smegmatis* mc^2155 or *M. abscessus* strains GD273 and GD286.
776 Plaque assays were performed at least twice with similar results.
777
778 **Figure 4. TPPs are essential for BPs_Δ*33*HTH_HRM10 to lyse *M. abscessus*. A**.
779 Representation of the *M. abscessus* TPP locus showing mutations affecting the clinical strains
780 studied. **B**. Phages were spotted as ten-fold serial dilutions onto clinical strains, resistant
781 mutants and complemented strains. Plates were incubated 2-3 days at 37° C prior to imaging.
782 The assay was repeated at least three times and a representative experiment is shown. **C**.TLC
783 analysis of total lipids extracted from *M. abscessus* clinical strains (GD22 and GD180),
784 spontaneous resistant mutants (RM) and complemented strains (::C). Eluent: $CHCl_3/CH_3OH$
785 (90:10, v/v). Anthrone was sprayed on the plates to visualize the lipid profile and followed by
786 charring. **D**. Liquid growth of the strains with or without BPs_Δ*33*HTH_HRM10 or
787 BPs_Δ*33*HTH_HRM10 mCherry (MOI 10) monitored every 6 hours for 6 days at 37° C in

788 7H9/OADC supplemented with 1 mM $CaCl_2$. Data are plotted as the median of three
789 independent experiments made in triplicates ± interquartile range. Statistical analysis conducted
790 to compare the differences at 144h between each strain: ns, P ≥ 0.05, * P ≤ 0.05, ** P ≤ 0.01,
791 *** P ≤ 0.001**** P ≤ 0.0001. **E**. Representative fields of *M. abscessus* clinical strains infected
792 with BPs_Δ*33*HTH_HRM10 mCherry (MOI 10) for 4 hours at 37° C prior to fixation. Infected
793 bacilli appear in red. **F**. Flow cytometry data are represented as dot plot show the percentage of
794 bacilli infected with the BPs_Δ*33*HTH_HRM10 mCherry fluorophage relative to the study
795 population.
796
797 **Figure 5. TPPs are also required for infection of *M. smegmatis* by phages BPs and**
798 **Muddy. A**. Tenfold serial dilutions of phages (as indicated on left) were spotted onto solid media
799 with *M. smegmatis* mc^2155, Δ*pks*, Δ*papA3* or Δ*fadD23* as indicated. Plaque assays were
800 performed at least twice with similar results. **B**. TLC analysis of total lipids extracted from wild-
801 type *M. smegmatis*, three TPP-deficient mutants and the corresponding complemented strains.
802 Eluent: $CHCl_3/CH_3OH$ (90:10, v/v). TLC was revealed by spraying anthrone on the plate,
803 followed by charring. **C**. Adsorption of phages BPs_Δ*33*HTH_HRM10, phKSW1 and ZoeJΔ*43-*
804 *45* on *M. smegmatis* strains mc^2155 and Δ*pks* as indicated by the percentage of unadsorbed
805 phages remaining in supernatant at different times after infection. Assays were performed in
806 triplicate at least twice with similar results and a representative experiment is shown. Data are
807 represented as the mean ±SD. Other replicates are shown in Figure S5. **D**. A panel of phages
808 from various genetic clusters were tenfold serially diluted and spotted onto *M. smegmatis*
809 mc^2155 and Δ*pks.* Phage names are shown with their cluster/subcluster designation in
810 parentheses.
811
812 **Figure 6. Evidence for additional phage resistance mechanisms. A.** Recovery of *M.*
813 *abscessus* GD01 transposon mutants resistant to phages BPs, phKSW1, Muddy, and

814 Muddy_REM1. A culture of an *M. abscessus* GD01 transposon library (GD01 Tn Lib) containing
815 approximately 10^6 CFU was plated onto phage-seeded plates as indicated. **B**. Phage infection
816 profiles of resistant mutants. Ten-fold serial dilutions of phages BPs∆*33*HTH_HRM10 ("BPs"),
817 phKSW1, Muddy, Muddy_REM1 and ZoeJ∆*43-45* ("ZoeJ") (as indicated at the left) were spotted
818 onto lawns of *M. abscessus* GD01 or mutants isolated as resistant to TPP-independent phages
819 phKSW1 and Muddy_REM1. Mutant designations indicate they are Tn insertions (Tn), the
820 phage used for mutant selection (i.e. phKSW1 or Muddy_REM1), and the mutant number (e.g.
821 RM1, RM2 etc). Where siblings are suspected (Table S1) only one representative is shown. **C**.
822 Organization of a putative candidate phage-inducible chromosomal island (PICI) in *M.*
823 *abscessus* GD01. The satellite region is defined by the *attL* and *attR* attachment sites resulting
824 from site-specific integration at a tRNA-Leu gene (GD01 coordinates 1158039 to 1170246). It
825 contains several phage-related genes (green boxes) with the putative functions indicated. At the
826 extreme right-hand end of the PICI, a gene (locus tag EXM25_05825) carries a DUF4145
827 domain implicated in phage defense in other systems. Four mutants contain a Tn insertion at
828 the site indicated by the vertical arrow. **D**. TLC analysis of total lipids extracted from *M.*
829 *abscessus* GD01 and transposon mutants isolated as resistant to TPP-independent phages. **E**.
830 Adsorption of BPs∆*33*HTH_HRM10 and phKSW1 to GD01Tn_phKSW1_RM1 (blue, top panels)
831 and to GD01Tn_phKSW1_RM2 (green, bottom panels). Adsorption to GD01 performed in
832 parallel is shown in black. The proportions of phage particles remaining in solution are shown at
833 different times after infection. Assays were performed in duplicate twice and the mean is
834 displayed; error bars represent one standard deviation.
835
836

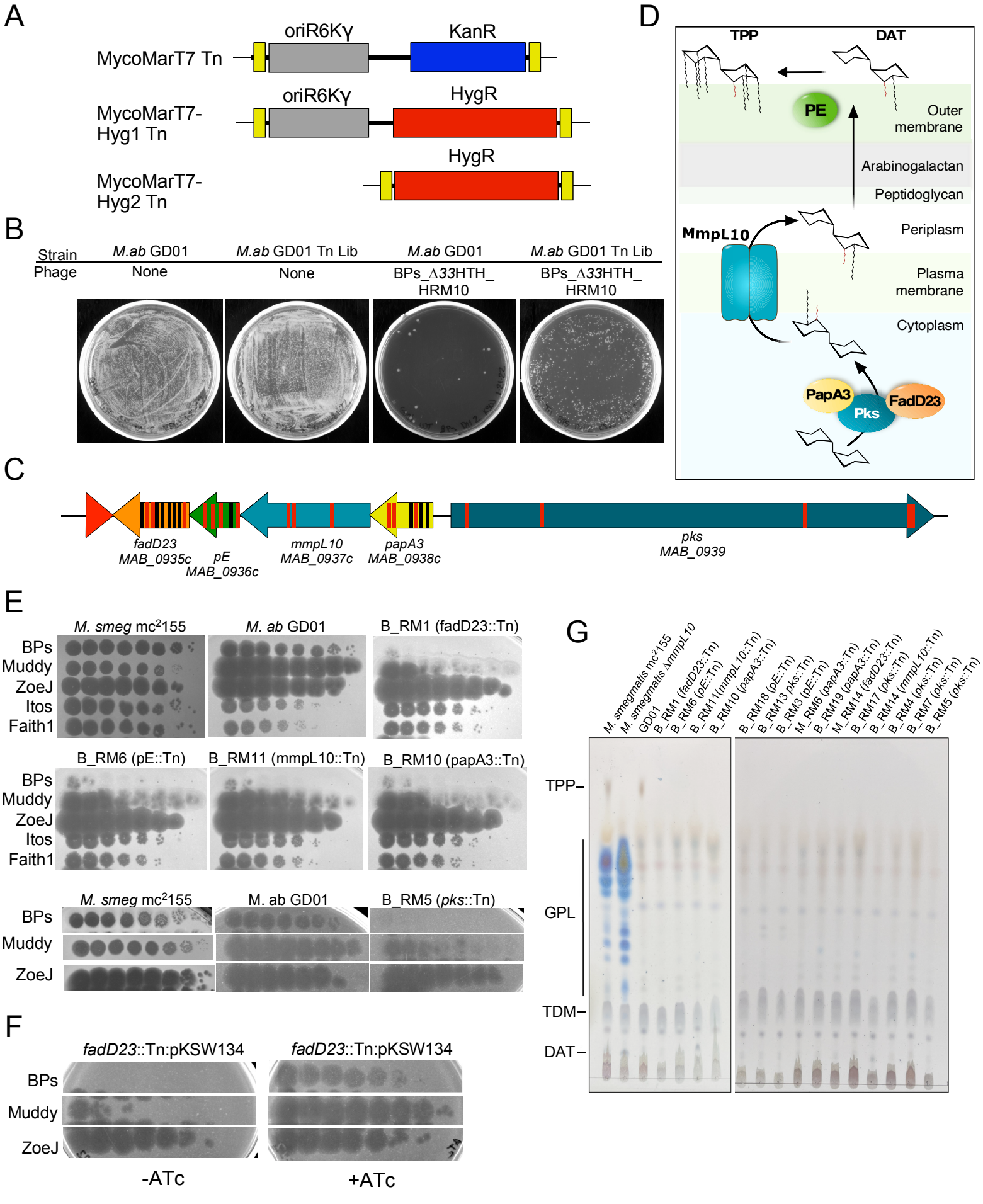
A
MycoMarT7 Tn
oriR6Kγ
KanR
MycoMarT7-Hyg1 Tn
oriR6Kγ
HygR
MycoMarT7-Hyg2 Tn
HygR
B
Strain
Phage
M.ab GD01
None
M.ab GD01 Tn Lib
None
M.ab GD01
BPs_Δ33HTH_HRM10
M.ab GD01 Tn Lib
BPs_Δ33HTH_HRM10
C
fadD23
MAB_0935c
pE
MAB_0936c
mmpL10
MAB_0937c
papA3
MAB_0938c
pks
MAB_0939
D
TPP
DAT
PE
Outer membrane
Arabinogalactan
Peptidoglycan
MmpL10
Periplasm
Plasma membrane
Cytoplasm
PapA3
Pks
FadD23
E
M. smeg mc²155
M. ab GD01
B_RM1 (fadD23::Tn)
BPs
Muddy
ZoeJ
Itos
Faith1
B_RM6 (pE::Tn)
B_RM11 (mmpL10::Tn)
B_RM10 (papA3::Tn)
M. smeg mc²155
M. ab GD01
B_RM5 (pks::Tn)
F
fadD23::Tn:pKSW134
fadD23::Tn:pKSW134
-ATc
+ATc
G
M. smegmatis mc²155
M. smegmatis ΔmmpL10
GD01
B_RM1 (fadD23::Tn)
B_RM6 (pE::Tn)
B_RM11(mmpL10::Tn)
B_RM10 (papA3::Tn)
B_RM18 (pE::Tn)
B_RM13 pks::Tn)
B_RM3 (pE::Tn)
M_RM6 (papA3::Tn)
B_RM19 (papA3::Tn)
M_RM14 (fadD23::Tn)
B_RM17 (pks::Tn)
B_RM14 (mmpL10::Tn)
B_RM4 (pks::Tn)
B_RM7 (pks::Tn)
B_RM5 (pks::Tn)
TPP
GPL
TDM
DAT

Figure 1

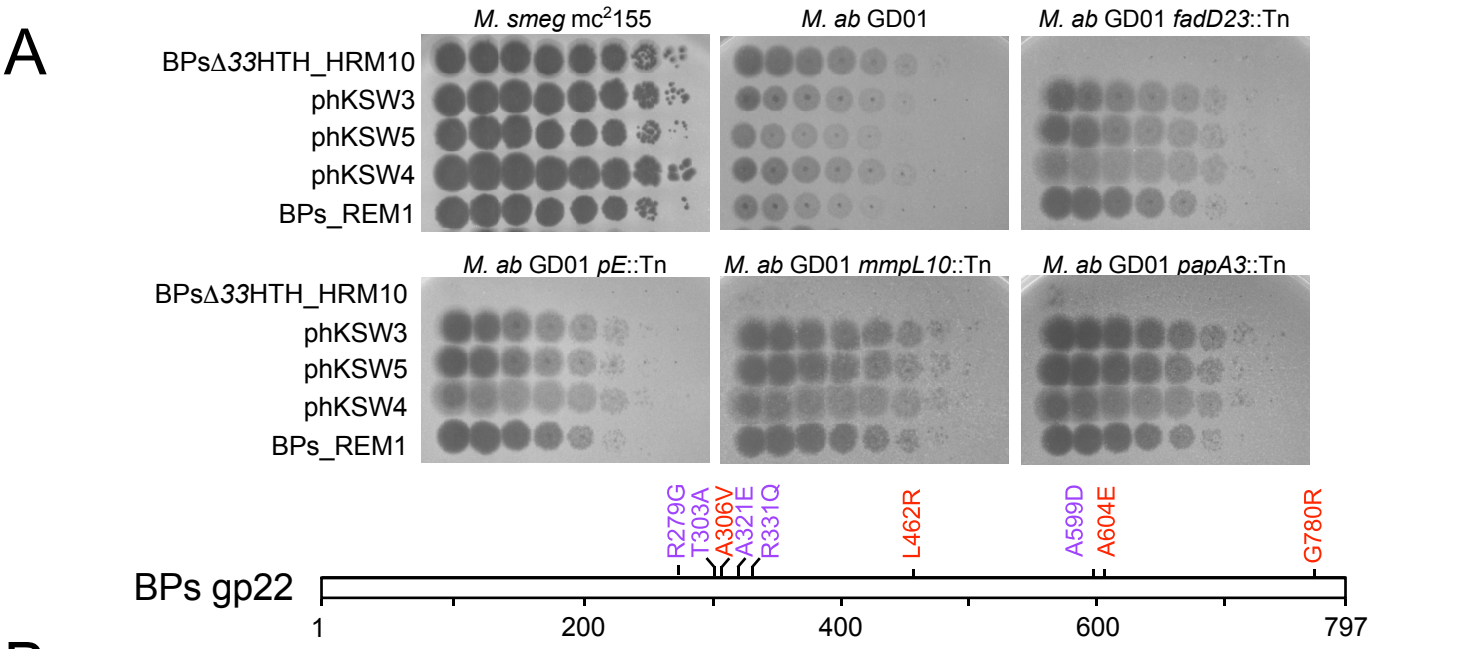
A
M. smeg mc²155
M. ab GD01
M. ab GD01 fadD23::Tn
BPsΔ33HTH_HRM10
phKSW3
phKSW5
phKSW4
BPs_REM1
M. ab GD01 pE::Tn
M. ab GD01 mmpL10::Tn
M. ab GD01 papA3::Tn
BPs gp22
R279G
T303A
A306V
A321E
R331Q
L462R
A599D
A604E
G780R
1
200
400
600
797

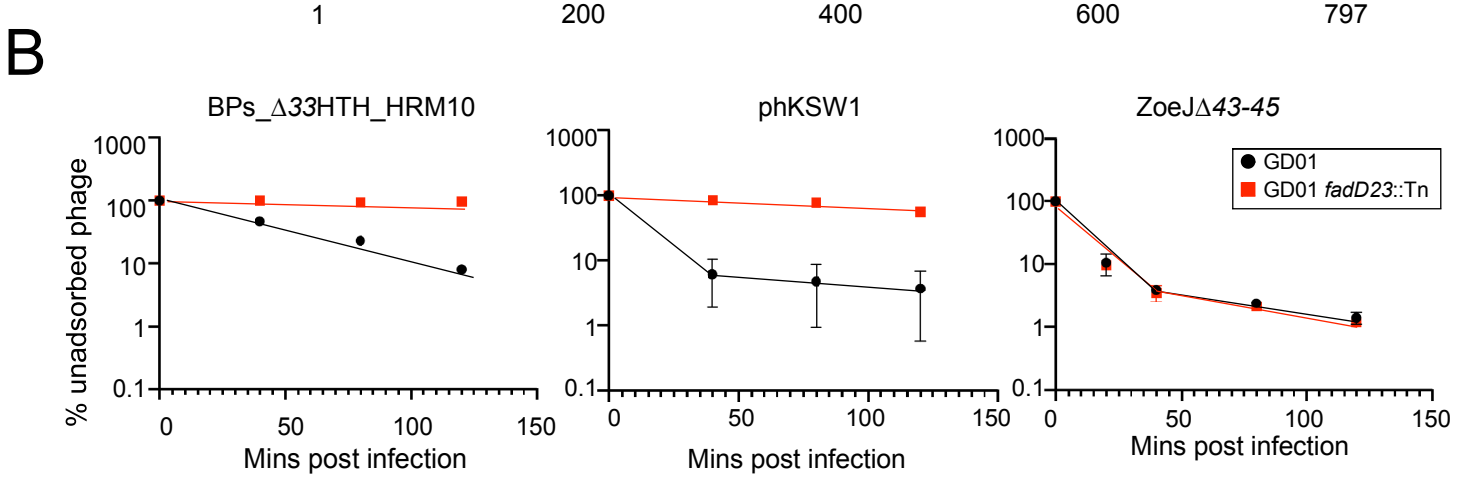
B
BPs_Δ33HTH_HRM10
phKSW1
ZoeJΔ43-45
% unadsorbed phage
1000
100
10
1
0.1
0
50
100
150
Mins post infection
GD01
GD01 fadD23::Tn

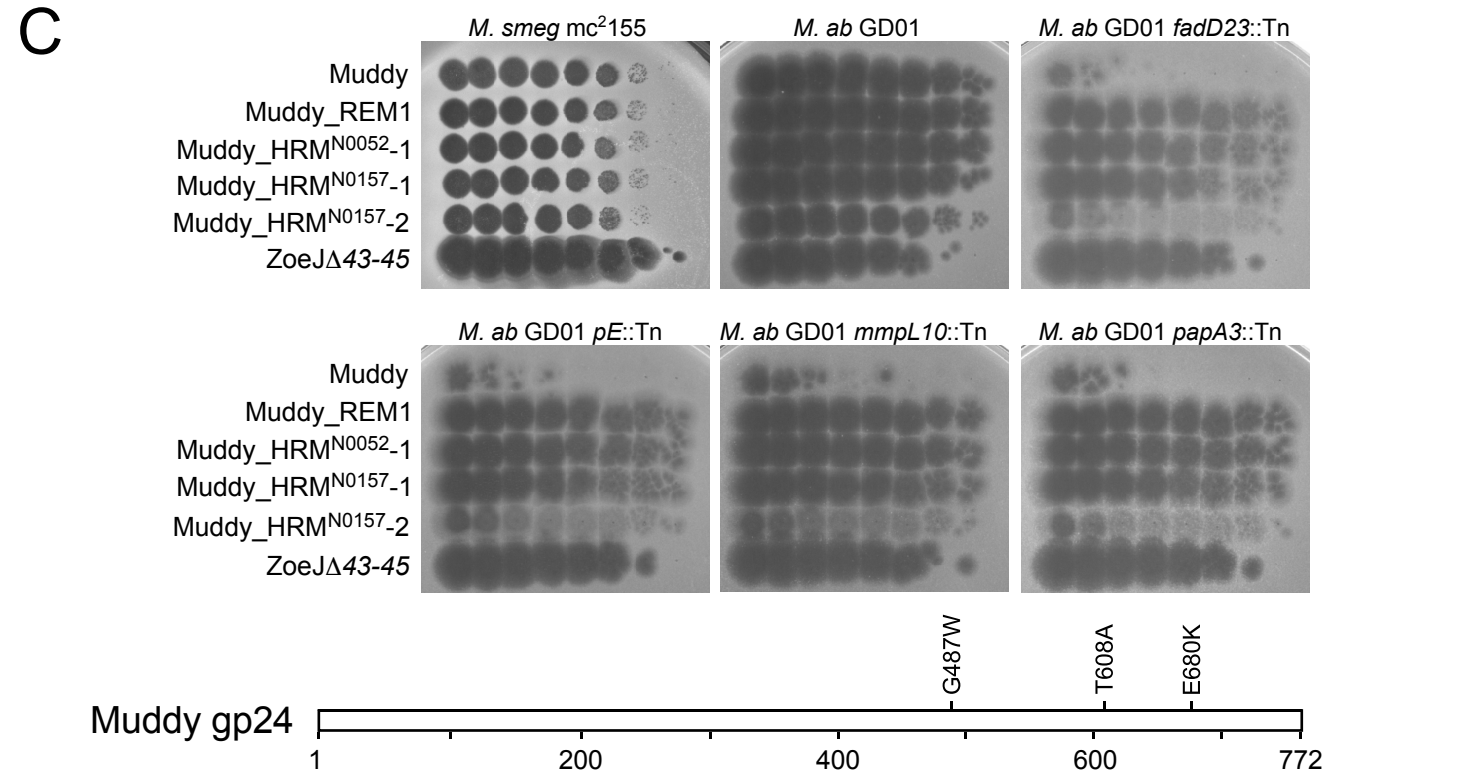
C
M. smeg mc²155
M. ab GD01
M. ab GD01 fadD23::Tn
Muddy
Muddy_REM1
Muddy_HRM^N0052-1
Muddy_HRM^N0157-1
Muddy_HRM^N0157-2
ZoeJΔ43-45
M. ab GD01 pE::Tn
M. ab GD01 mmpL10::Tn
M. ab GD01 papA3::Tn
Muddy gp24
G487W
T608A
E680K
1
200
400
600
772

Figure 2

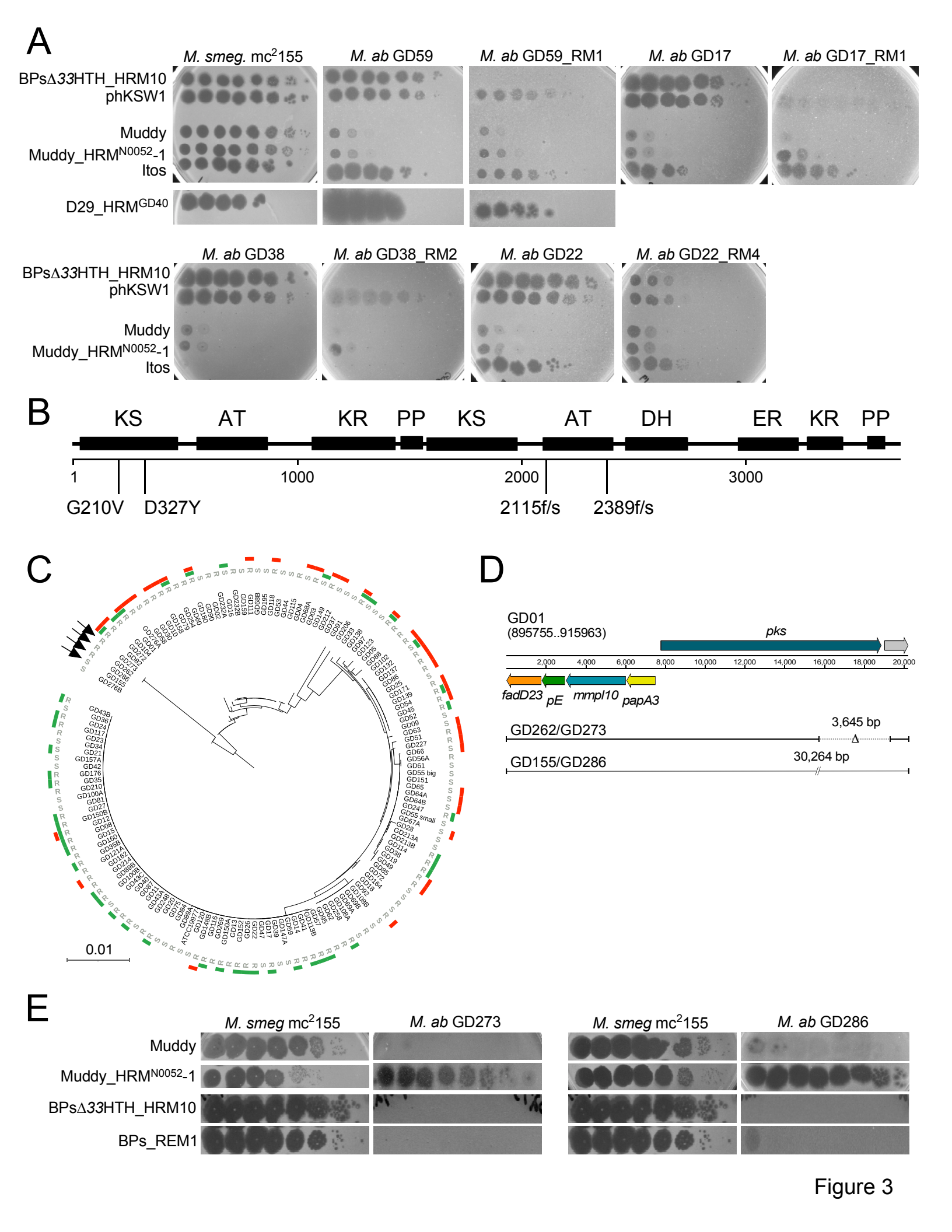
A
M. smeg. mc2155
M. ab GD59
M. ab GD59_RM1
M. ab GD17
M. ab GD17_RM1
BPsΔ33HTH_HRM10
phKSW1
Muddy
Muddy_HRMN0052-1
Itos
D29_HRMGD40
M. ab GD38
M. ab GD38_RM2
M. ab GD22
M. ab GD22_RM4
BPsΔ33HTH_HRM10
phKSW1
Muddy
Muddy_HRMN0052-1
Itos
B
KS
AT
KR
PP
KS
AT
DH
ER
KR
PP
1
1000
2000
3000
G210V
D327Y
2115f/s
2389f/s
C
0.01
D
GD01
(895755..915963)
pks
2,000
4,000
6,000
8,000
10,000
12,000
14,000
16,000
18,000
20,000
fadD23
pE
mmpl10
papA3
GD262/GD273
3,645 bp
GD155/GD286
30,264 bp
E
M. smeg mc2155
M. ab GD273
M. smeg mc2155
M. ab GD286
Muddy
Muddy_HRMN0052-1
BPsΔ33HTH_HRM10
BPs_REM1

Figure 3

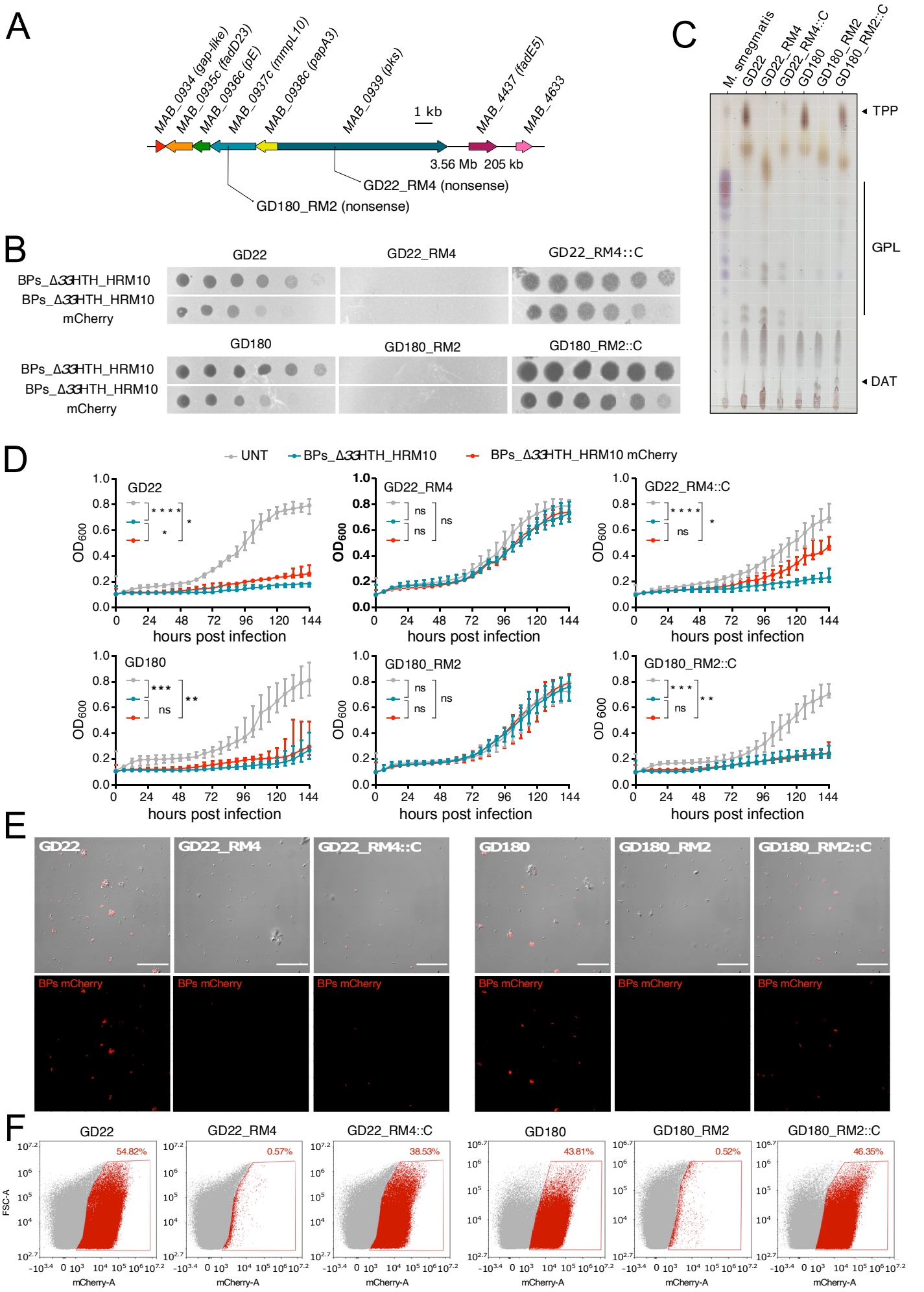
A
MAB_0934 (gap-like)
MAB_0935c (fadD23)
MAB_0936c (pE)
MAB_0937c (mmpL10)
MAB_0938c (papA3)
MAB_0939 (pks)
1 kb
MAB_4437 (fadE5)
MAB_4633
3.56 Mb 205 kb
GD22_RM4 (nonsense)
GD180_RM2 (nonsense)
B
GD22
GD22_RM4
GD22_RM4::C
BPs_Δ33HTH_HRM10
BPs_Δ33HTH_HRM10
mCherry
GD180
GD180_RM2
GD180_RM2::C
BPs_Δ33HTH_HRM10
BPs_Δ33HTH_HRM10
mCherry
C
M. smegmatis
GD22
GD22_RM4
GD22_RM4::C
GD180
GD180_RM2
GD180_RM2::C
TPP
GPL
DAT
D
UNT
BPs_Δ33HTH_HRM10
BPs_Δ33HTH_HRM10 mCherry
GD22
GD22_RM4
GD22_RM4::C
GD180
GD180_RM2
GD180_RM2::C
OD600
hours post infection
ns
E
GD22
GD22_RM4
GD22_RM4::C
GD180
GD180_RM2
GD180_RM2::C
BPs mCherry
F
GD22
GD22_RM4
GD22_RM4::C
GD180
GD180_RM2
GD180_RM2::C
54.82%
0.57%
38.53%
43.81%
0.52%
46.35%
FSC-A
mCherry-A

Figure 4

A

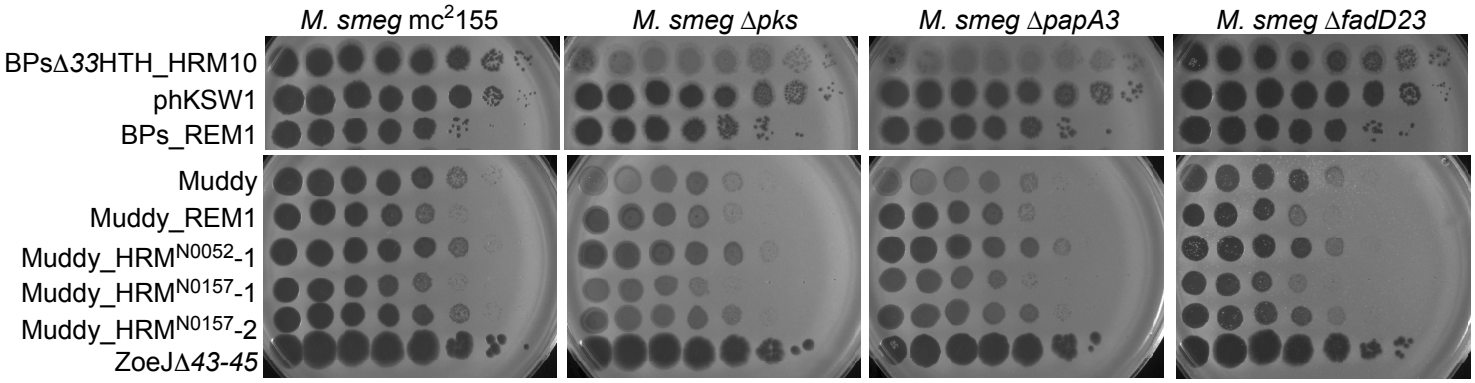

B

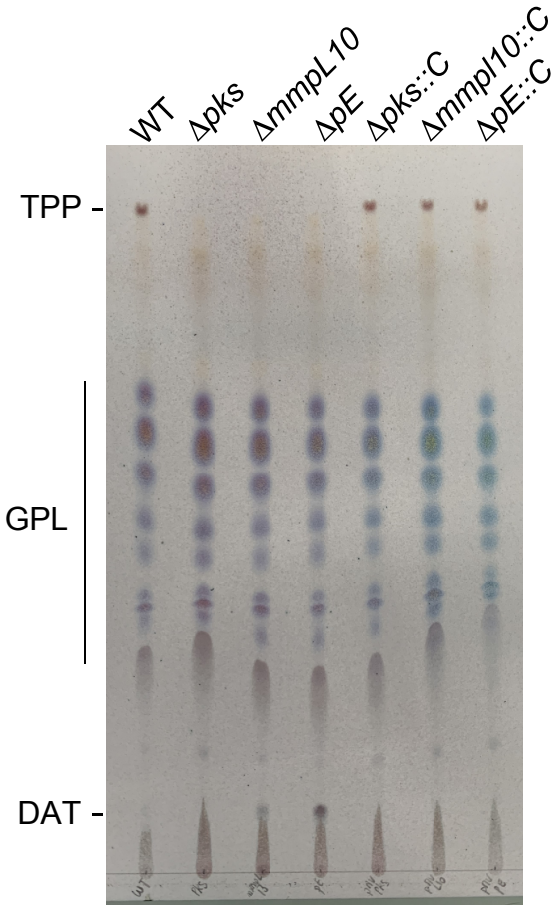

D

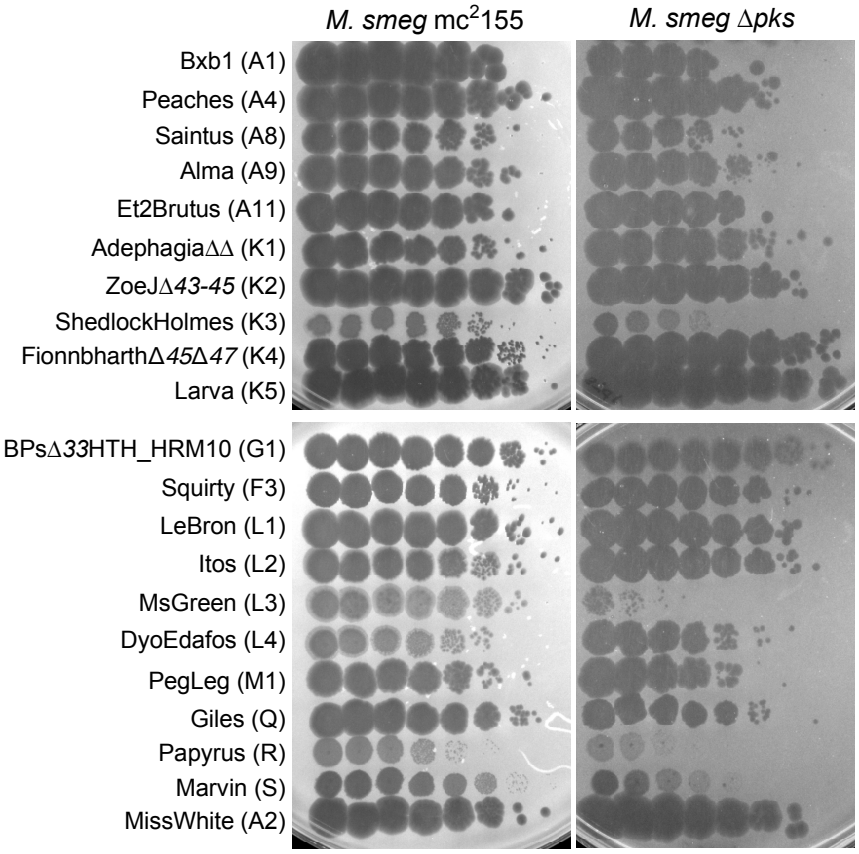

C

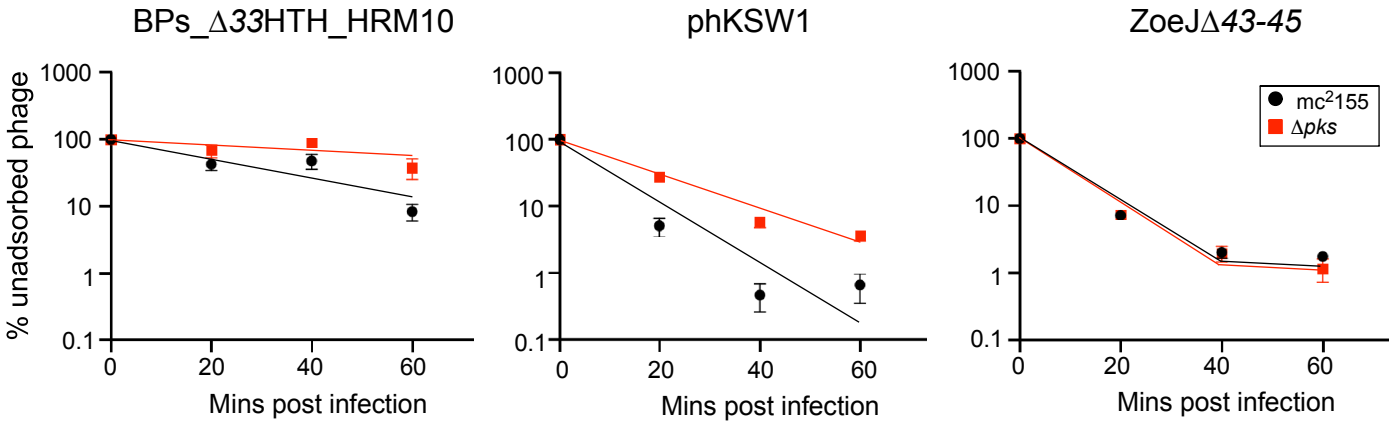

Figure 5

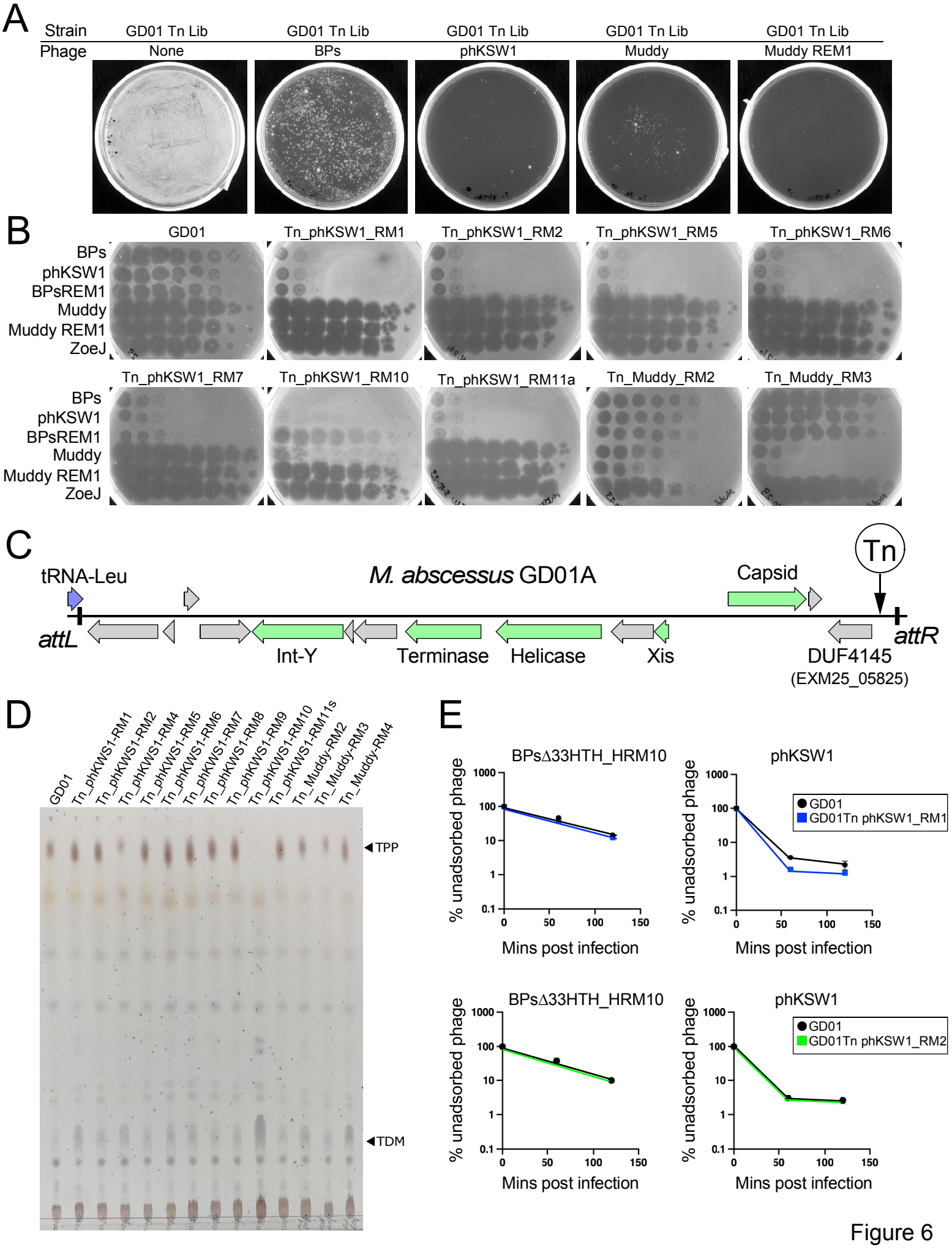
A
Strain
Phage
GD01 Tn Lib
None
BPs
phKSW1
Muddy
Muddy REM1
B
GD01
Tn_phKSW1_RM1
Tn_phKSW1_RM2
Tn_phKSW1_RM5
Tn_phKSW1_RM6
Tn_phKSW1_RM7
Tn_phKSW1_RM10
Tn_phKSW1_RM11a
Tn_Muddy_RM2
Tn_Muddy_RM3
BPs
phKSW1
BPsREM1
Muddy
Muddy REM1
ZoeJ
C
tRNA-Leu
M. abscessus GD01A
Capsid
Tn
attL
attR
Int-Y
Terminase
Helicase
Xis
DUF4145
(EXM25_05825)
D
GD01
Tn_phKWS1-RM1
Tn_phKWS1-RM2
Tn_phKWS1-RM4
Tn_phKWS1-RM5
Tn_phKWS1-RM6
Tn_phKWS1-RM7
Tn_phKWS1-RM8
Tn_phKWS1-RM9
Tn_phKWS1-RM10
Tn_phKWS1-RM11s
Tn_Muddy-RM2
Tn_Muddy-RM3
Tn_Muddy-RM4
TPP
TDM
E
BPsΔ33HTH_HRM10
phKSW1
% unadsorbed phage
Mins post infection
GD01
GD01Tn phKSW1_RM1
GD01Tn phKSW1_RM2

Figure 6